Acta Applicandae Mathematicae **57:** 287–338, 1999.

On the Dido Problem and Plane Isoperimetric Problems

ANDREI A. AGRACHEV* and JEAN-PAUL A. GAUTHIER
Laboratoire de Topologie, UMR 5584, University of Burgandy, BP 400, 21011, Dijon Cedex, France

(Received: 4 April 1999)

Abstract. This paper is a continuation of a series of papers, dealing with contact sub-Riemannian metrics on R^3. We study the special case of contact metrics that correspond to isoperimetric problems on the plane. The purpose is to understand the nature of the corresponding optimal synthesis, at least locally. It is equivalent to studying the associated sub-Riemannian spheres of small radius. It appears that the case of generic isoperimetric problems falls down in the category of generic sub-Riemannian metrics that we studied in our previous papers (although, there is a certain symmetry). Thanks to the classification of spheres, conjugate-loci and cut-loci, done in those papers, we conclude immediately. On the contrary, for the Dido problem on a 2-d Riemannian manifold (i.e. the problem of minimizing length, for a prescribed area), these results do not apply. Therefore, we study in details this special case, for which we solve the problem generically (again, for generic cases, we compute the conjugate loci, cut loci, and the shape of small sub-Riemannian spheres, with their singularities). In an addendum, we say a few words about: (1) the singularities that can appear in general for the Dido problem, and (2) the motion of particles in a nonvanishing constant magnetic field.

Mathematics Subject Classifications (1991): Primary: 05C38, 15A15; Secondary: 05A15, 15A18.

Key words: sub-Riemannian geometry, optimal control.

1. Introduction

1.1. MOTIVATION: 2-D ISOPERIMETRIC PROBLEMS AND THE DIDO PROBLEM

In this paper, we consider the *very elementary* situation of a *general isoperimetric problem* on a 2-dimensional Riemannian manifold. Moreover, in most of the paper, we remain at the *local* level. Despite the apparent simplicity of the context, we obtain new and interesting results.

We work in the C^∞ category. (M, g) is an oriented 2-d Riemannian structure. Almost everywhere in the paper, it will just be a germ at $q_0 \in M$ of such a structure. We are given on (M, g) a 2-form, $\eta = (\text{Volume})\psi$, and we consider the following class of isoperimetric problems, (M, g, η):

$q_{0,}q_1 \in M$ are fixed, together with a smooth curve $\tilde{\gamma}\colon [0, 1] \to M, \tilde{\gamma}(0) = q_0, \tilde{\gamma}(1) = q_1$, and we are looking for curves $\gamma\colon [0, 1] \to M,\ \gamma(0) = q_1,\ \gamma(1) = q_0$, with minimal Riemannian length l, such that the value A of the integral $\int_\Omega \eta$ is

* Also at Steklov Mathematical Institute, 8 ul. Gubkina, GSP1, Moscow, 117966, Russia.

prescribed, where Ω is the domain encircled by γ and $\tilde{\gamma}$. This problem is referred to as the "isoperimetric problem", or problem (I).

If $\psi = 1$, (I) is just the dual formulation of the classical isoperimetric problem (called the Dido problem) which consists of maximizing the area, for prescribed length. It can be shown that both formulations are equivalent, at least at the local level.

Note 1. This Dido problem is also sometimes named the *Pappus Problem* (see for instance Carathéodory [8, pp. 366–370]) in honor of the Greek mathematician who solved it in the particular case of the Euclidean metric on the plane.

Even for the *Dido problem at the local level* (i.e. small areas, or small perimeters), some interesting phenomena appear, as we shall show.

Just as an example, let us state a result and a corollary which show what can happen. These results are simple consequences of the main theorems in this paper.

$q_0 \in M$ denotes the pole, α denotes a certain primitive of the volume form, and, A denotes the (small) prescribed value of the integral $\int_0^1 \alpha(\dot{\gamma}(\tau))\,d\tau$. We will treat only the case $A > 0$, The case $A < 0$ is similar and is obtained by reversing orientation.

Let us set $h = \sqrt{A/\pi}$. Let $k(q_0)$ denote the Gaussian curvature of (M, g) at q_0.

The successive covariant derivatives $\nabla^j k$ are covariant symmetric tensor fields of degree j on M and they can be decomposed under the action of the structural group SO(2) of TM on the fibers of the corresponding vector bundles, into isotypic components relative to successive powers $e^{li\varphi}$ of the basic character $e^{i\varphi}$, $i = \sqrt{-1}$:

$$\nabla^j k(q_0) = \sum_{l=0}^{j} \left(\nabla_l^j k(q_0)\right). \tag{1.1}$$

In particular, $\nabla^2 k(q_0)$ is a quadratic form, $\nabla^2 k(q_0) = \nabla_0^2 k(q_0) + \nabla_2^2 k(q_0)$, where $\nabla_0^2 k(q_0) = \frac{1}{2}\mathrm{trace}_g(\nabla^2 k(q_0))\ g(q_0)$, and $\nabla_2^2 k(q_0) = 0$ iff the discriminant $\mathrm{discr}_g(\nabla^2 k(q_0)) = 0$. $\nabla^3 k(q_0)$ is cubic, $\nabla^3 k(q_0) = \nabla_1^3 k(q_0) + \nabla_3^3 k(q_0)$.

Let us consider the following vectors V_1, V_2^1, V_2^2, V_3^1, V_3^2, V_3^3 in $T_{q_0}M$:

(1) V_1 is the vector which is normal to the gradient of k at q_0 with length $\pi/4\ |\mathrm{grad}\, k|_{q_0}$, and the frame $(\mathrm{grad}\, k, V_1)_{q_0}$ is direct,

(2) V_2^i are the vectors in the direction where the quadratic form $\nabla_2^2 k(q_0)$, reaches its maximum $\tilde{r}_2$ on the unit circle, with length $(\pi/2)\tilde{r}_2$,

(3) V_3^j are the vectors that are normal to the directions I_1, I_2, I_3 where the cubic form $\nabla_3^3 k(q_0)$ reaches its maximum $\tilde{r}_{32}$ over the unit circle, with length $(3\pi/8)\tilde{r}_{32}$, and the frames (I_j, V_3^j) are direct, $j = 1, 2, 3$.

The "cut locus" Cut $L(h)$ corresponding to the prescribed value h is defined as the subset of M formed by the points q_1 that are joined to q_0 by several (*not unique*) minimum length trajectories.

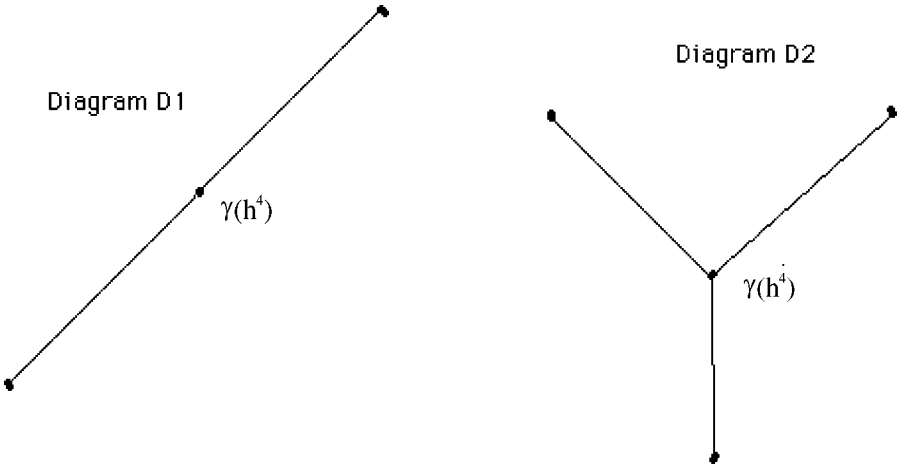

Figure 1. The generic Cut Loci.

THEOREM 1.1 (Illustration of further results). *For a germ of Riemannian metric at q_0 and for h small enough, the following statements hold.*

There exists a germ of smooth curve $\gamma(t)$ at q_0 such that $\mathrm{d}\gamma(t)/\mathrm{d}t(q_0) = V_1$, and:

(1) *if $\nabla_2^2 k(q_0) \neq 0$, then, $\mathrm{Cut}\, L(h)$ is a tree graph formed by two semi-open smooth curve segments issued from the point $\gamma(h^4)$. The direction of these two segments is V_2^i, their length has asymptotics $h^5|V_2^i|$;*

(2) *if $\nabla_2^2 k(q_0) = 0$ but $\nabla_3^3 k(q_0) \neq 0$, then, $\mathrm{Cut}\, L(h)$ is a tree graph formed by three semi-open smooth curve segments issued from the same point $\gamma(h^4)$. The direction of these segments is V_3^i, their length has asymptotics $h^6|V_3^i|$.*

Figure 1 shows two diagrams, D_1 and D_2, which give the shape of the generic cut loci. Consequently:

COROLLARY 1.2 (For generic Riemannian metrics g over M). *There are two types of points $q_0 \in M$: $q_1 \in M$ denotes any point sufficiently close to q_0, γ: $[0, 1] \to M$, $\gamma(0) = q_0$, $\gamma(1) = q_1$, denotes any curve issued from q_0, with prescribed value A of the integral $\int_0^1 \alpha(\dot\gamma(\tau))\,\mathrm{d}\tau$, $|A|$ sufficiently small. Then:*

(1) *if $\nabla_2^2 k(q_0) \neq 0$ (generic points), there are exactly one or two optimal curves γ,*

(2) *if $\nabla_2^2 k(q_0) = 0$ (isolated points), there are points q_1 with 3 optimal curves γ from q_0 to q_1.* (*Optimal means minimum length.*)

The triple point of case 2 is just the point $\gamma(h^4)$, all other points of the semi-open curve segments being double.

Note 2. It follows from the theory of characteristic classes (see [17], Chapter 40, page 204, for instance) that if M is a compact manifold, and the Euler characteristic $\varkappa(M)$ is nonzero, there are always isolated points of the second type: $\nabla_2^2 k$

defines a field of quadratic forms with signature 1 on the complement in M of the set of these isolated points, and the sum of indices of the associated "field of line elements" is $2\,\varkappa(M)$.

In fact, our main purpose in this paper is to describe the shape of what is called (in terms of control theory) the local *optimal synthesis* for a generic isoperimetric problem and for the special case of the Dido problem. That is, for any fixed value of q_0, *we want to find all optimal curves from* q_0 *to* q_1, for all $|A|$ small enough, and for all q_1 close enough to q_0.

This Goal will be achieved in this paper. In the next Section 2, we will show that, for *generic* isoperimetric problems (M, g, η) the answer to this question is just an immediate consequence of the main results of a series of papers of ours ([2, 5, 9, 4]).

Unfortunately, for the very special case of the Dido problem, these arguments are not valid. We will solve this local Dido problem in Section 3, and show that mainly there is only a change of scale, but up to this change, the results are very similar to those of the generic isoperimetric (or sub-Riemannian) case. The main results are Theorem 3.7, Theorem 3.8.

We don't state the results precisely in terms of isoperimetric problems in this paper. We leave this to the reader: in fact, it is very natural and convenient to reformulate everything and state all results in terms of sub-Riemannian geometry.

1.2. REFORMULATION IN TERMS OF SUB-RIEMANNIAN GEOMETRY (ISOPERIMETRIC STRUCTURES, FIRST DEFINITION)

These considerations are classical. One can consult for instance the survey paper by Montgommery [15].

Let (M, g) be a 2-d Riemann metric (with orientation), and let $\pi\colon E \to M$ be a (circle or line) principal bundle over M. For instance, one can consider the (circle) principal bundle of oriented orthonormal frames over M.

The data (E, M, g, π, Δ) of such a principal bundle $\pi\colon E \to M$ over a Riemannian manifold (M, g), and a connection Δ on this principal bundle defines a sub-Riemannian structure over E in the obvious way: the underlaying distribution is the "horizontal space" Δ of the connection, and the sub-Riemannian metric g_E is the lift on Δ via π of the Riemann metric on M : $g_E = \pi_* g$.

DEFINITION 1.1. Such a structure (E, M, g, π, Δ) is called an isoperimetric structure.

An isoperimetric structure is a *special sub-Riemannian structure* over E, since such a structure is invariant under the action of the (circle or line) structure group of the bundle π. It is very easy to check that the sub-Riemannian structure obtained in this way is a *contact* structure if and only if *the curvature form of the connection is nonvanishing*.

DEFINITION 1.2. If the curvature form of the connection is a constant multiple of the lift of the volume form of (M, g), then we call this structure a *Dido structure*.

If we stay at the local level on E (small prescribed areas, or small prescribed perimeters, for isoperimetric problems), then it doesn't make any difference to consider either circle or line groups. Also, a Dido structure is *completely determined by the underlaying Riemannian structure* (plus the nonsignificant constant appearing in the definition).

The problem of "optimal synthesis" for isoperimetric problems is equivalent to the problem of computing the "Cost function" $C(p_1) = d(p_0, p_1)$, where d is the sub-Riemannian distance over E. The level surfaces of this cost functions are just the sub-Riemannian spheres. It turns out that (in contrast with Riemannian geometry) this cost function and its level surfaces, the spheres, are not smooth, even locally. They have singularities, that should be described. This program has already been carried out for generic germs of contact sub-Riemannian metrics, in our papers ([2, 5, 9, 4]).

Note 3. This work has also been done in the noncontact "flat Martinet case", in the papers [3, 10], leading to very interesting results: the distance function, for the most elementary noncontact analytic isoperimetric structure, is not subanalytic. On the contrary, it follows from our papers that, in the contact case it is subanalytic.

As we shall see in the next section, generic isoperimetric structures have the same classification as generic sub-Riemannian structures: the invariants leading to this classification (there are two, mainly), are nondegenerate. *It is the main purpose of this paper to make the same generic classification for Dido structures.*

Also, in this paper, we will give, in the Dido case, more details about computations of the cut locus, and more generally the self-intersections of the wave fronts. This was partly done for general sub-Riemannian metrics in [2].

1.3. COMPLEMENTS

In our last Section 4, we will briefly mention two interesting complements. We will deal with the motion of charged particles in a nonvanishing magnetic field ψ. The motion of a particle with charge c is given by the equation:

$$k_g(z(s)) = c\ \psi(z(s)), \tag{1.2}$$

where $k_g(z(s))$ denotes the geodesic curvature of the curve $z(s)$.

It appears (see Section 4) that the trajectories of the motion are exactly the geodesics of an underlaying contact isoperimetric sub-Riemannian metric. If the magnetic field is constant, it is a Dido structure. Some problems of collision of particles with the same charge are very similar to the problem of computing the cut locus of a point for the metric. In the context of Riemannian geometry, at the local

level, the cut locus of the pole q_0 is empty. This is never the case in sub-Riemannian geometry, and in particular this is never the case for general isoperimetric metrics or for the Dido metrics. On the same way, there will be a locus where collision of particles occur, arbitrarily close to the origin.

It is rather strange that this locus is very different from the cut-locus: in particular, its size has not the same order (although the caustic is the same).

The other problem we will address in this last section is the following: the sub-Riemannian conjugate locus of the pole q_0 also, has q_0 in its closure (similarly to the cut locus). As we shall see, this conjugate locus is a certain surface, with a certain number of cuspidal lines. For generic Dido structures (generic Riemannian metrics), this number is 4 or 6. We will show that for more degenerate Riemann metrics, it can be arbitrarily large. Also, the number of branches of the cut locus can be arbitrarily large, provided that the Riemannian metric is flatter and flatter in some sense at the pole.

2. Preliminaries, Notations, Study of Generic Isoperimetric Structures

CONVENTION. All along the remaining of the paper, the notation $o(a_1, \dots, a_p)$ means a function of all variables under consideration, which is in the ideal $\Im$ generated by $a_1, \dots, a_p$. $o^k(a_1, \dots, a_p)$ means an element of $\Im^k$.

(E, Δ, g) denotes a sub-Riemannian metric over the 3-d manifold E. Δ is the underlaying distribution, and $g\colon\ \Delta \to R^+$ is the metric.

2.1. CHARACTERISTIC VECTOR FIELD

Assume that Δ is contact. There is a (unique up to orientation) one form α on E such that:

$$\begin{aligned} \operatorname{Ker}\alpha &= \Delta, \\ d\alpha_{|\Delta} &= \text{Volume}. \end{aligned} \tag{2.1}$$

There is also a (unique up to orientation) vector field v, called the *characteristic vector field*, such that:

$$\alpha(v) = 1,\ i_v(d\alpha) = 0, \tag{2.2}$$

or equivalently:

$$i_v(\alpha \wedge d\alpha) = d\alpha. \tag{2.3}$$

2.2. ISOPERIMETRIC STRUCTURE (SECOND DEFINITION)

DEFINITION 2.1. (E, Δ, g, X) is called an isoperimetric structure if (E, Δ, g) is a 3-d sub-Riemannian metric, X is a vector field on E, transversal to Δ, and the sub-Riemannian structure is invariant by the flow $\exp(tX)$ of the vector field X.

DEFINITION 2.2. A sub-Riemannian metric (E, Δ, g) is called a Dido metric (or a Dido structure) if it is contact and (E, Δ, g, ν) is an isoperimetric structure (ν being the characteristic vector field).

Note 4. (a) If (E, Δ, g, X) is a contact isoperimetric structure, X defines an orientation on Δ,

(b) If (E, Δ, g) is a Dido metric, then ν is defined up to orientation of Δ, but, if the orientation is reversed, ν is changed into $-\nu$, and the fact that (E, Δ, g) is ν-invariant is preserved.

If we are given an isoperimetric structure in the sense of Definition 1.1, then we have a sub-Riemannian structure over the principal bundle $\pi\colon E \to M$, which is invariant under the action of the vertical one parameter group of any element of the Lie algebra of the (circle or line) structure group. As we shall see, this isoperimetric structure is a Dido structure in the sense of the Definition 1.2 if and only if it is in the sense of the Definition 2.2.

2.3. EQUIVALENCE OF THE TWO DEFINITIONS (OF ISOPERIMETRIC AND DIDO STRUCTURES) AT THE LEVEL OF GERMS

Conversely, if $(E, \Delta, g, X)_{q_0}$ is a germ at q_0 of an isoperimetric structure in the sense of Definition 2.1, then:

(1) the quotient space $M = E/X$ of E by the foliation defined by the vector field X inherits a (germ of) Riemannian structure (with orientation if Δ is contact: the orientation on M is induced by the orientation on Δ defined by X).

(2) The germ $(E, \Delta, g, X)_{q_0}$ can be extended to a germ of a trivial principal (line) bundle over the germ $(M, g)_{\pi(q_0)}$, with a connection, the horizontal space of which is Δ.

If $(E, \Delta, g, X)_{q_0}$ is Dido, then $X = \nu$, and α defined in (2.1) is the form of the connection. Hence, the curvature form of the connection is the lift of the volume form.

Therefore, at the level of germs at least, the two definitions of isoperimetric and Dido structures are equivalent.

2.4. GEODESICS AND EXPONENTIAL MAPPING

Let us recall the basic facts about the sub-Riemannian geodesics and the exponential mapping *in the contact case*. In that case (contrarily to the isoperimetric "Martinet case" [3]), there is no abnormal geodesic. All geodesics are projections on E of trajectories of the Hamiltonian vector field $\mathbf{H}$ on T^*E associated to the Hamiltonian:

$$H(\psi) = \frac{1}{2} \sup_{v \in \Delta \setminus \{0\}} \left(\frac{\psi(v)}{\|v\|} \right)^2. \tag{2.4}$$

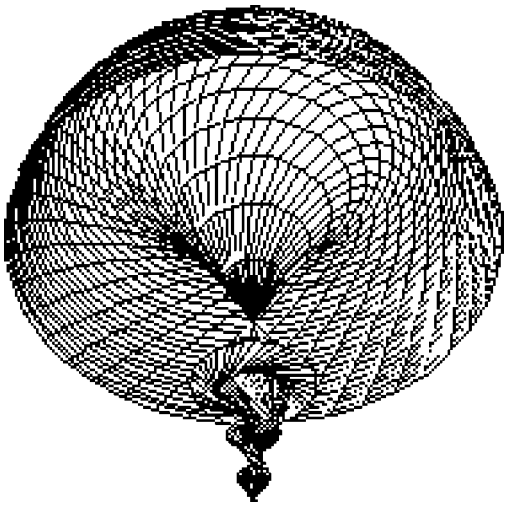

Figure 2. Half a Heisenberg wave front.

$H(\psi)$ is a positive semi-definite quadratic form on the fibers of $\pi_E\colon T^*E \to E$, the kernel of which is the annihilator of Δ.

If the metric is specified by an orthonormal frame field (F, G), then:

$$H(\psi) = \frac{1}{2}\big(\psi(F)^2 + \psi(G)^2\big). \tag{2.5}$$

In the isoperimetric situation, another more classical but equivalent characterization of geodesics can be given, in terms of the geodesic curvature of their projection on the quotient Riemannian manifold (see Section 4.2).

Let $H_{1/2} = H^{-1}(\frac{1}{2})$ be the level surface of H corresponding to geodesics that are parametrized by the arclength. Since the Hamiltonian (2.5) is homogeneous w.r.t. ψ, $H_{1/2}$ inherits the canonical contact structure of the projective cotangent bundle PT^*E. Let $\bar{C}_0 \subset T^*E$, $\bar{C}_0 = \pi_E^{-1}(q_0)$, $\pi_E\colon T^*E \to E$, and let C_0 be the cylinder $C_0 = \bar{C}_0 \cap H_{1/2}$. C_0 is a Legendre manifold for this contact structure, and the Hamiltonian flow preserves this contact structure.

The exponential mapping is the mapping:

$$\begin{aligned} &\varepsilon\colon C_0 \times R^+ \to E, \\ &(p, s) \to \pi_E \circ \exp\big(s\mathbf{H}(p)\big). \end{aligned} \tag{2.6}$$

2.5. CANONICAL SECTION

If $(E, \Delta, g, X)_{q_0}$ is a germ of an isoperimetric structure, $M = E/X$, then, there is a *canonical local smooth section* $s_{q_0}\colon M \to E$ through q_0, $(s_{q_0}(\pi_X(q_0)) = q_0)$: we consider on E the sub-Riemannian geodesics $\varepsilon(p, s)$, issued from q_0, which satisfy at q_0 the Pontriaguine's "transversality conditions" with respect to X, i.e.

$p(X(q_0)) = 0$ (see [16]), and which are parametrized by the arclength s. Since X is transversal to Δ, these geodesics are necessarily Hamiltonian (cannot be abnormal). *Our canonical section s_{q_0} is defined by*: $s_{q_0}(\pi_X(q)) = q'$, where q' is the unique point of E in $(\pi_X)^{-1} \circ \pi_X(q)$ which is of the form $\varepsilon(p, s)$. It is not hard to see that this construction defines a smooth section s_{q_0}. (Consult for instance our paper [4], but it is very easy.)

2.6. RELATION OF OUR DEFINITIONS WITH ISOPERIMETRIC PROBLEMS

If we have a germ of an isoperimetric structure (E, M, g, π, Δ), then, the curvature form $\bar{\eta}$ of the connection defines a 2-form η on M and hence an isoperimetric problem (M, g, η) in the sense of Section 1.1.

Conversely, if we consider a germ of an isoperimetric problem (M, g, η), then considering the trivial principal bundle $\pi\colon E = M \times R \to M$, $E = \{(q, A) | q \in M, A \in R\}$, and $\bar{\alpha} = dA + \pi_* \alpha$, where α is any primitive of the form η over M, we get a connection over E, defined by its form $\bar{\alpha}$. $\bar{\alpha}$ is defined up to any closed one-form dn over M:

$$\tilde{\alpha} = dA + \pi_*(\alpha + dn),$$

corresponds to the same isoperimetric problem.

Also, if two isoperimetric structures $(E, M, g, \pi, \bar{\Delta})$ and $(E, M, g, \pi, \tilde{\Delta})$ define the same isoperimetric problem over (M, g) then, their connection forms $\bar{\alpha}, \tilde{\alpha}$ differ locally from $\pi_* dn$, the pull-back of a closed one-form dn over M. The fiber mapping $(q, A) \to (q, A + n(q))$ is an isomorphism of these isoperimetric structures.

Let $\bar{q}_0 = (q_0, 0) \in M \times R$, and let the germ $(E = M \times R, M, g, \pi, \Delta)_{\bar{q}_0}$ be given. Then, there is a unique choice of the function n for the image $s_{\bar{q}_0}(M)$ of M by the canonical section $s_{\bar{q}_0}$ (defined in Section 2.5) be the set $s_{\bar{q}_0}(M) = \{(q, 0) \mid q \in M\}$.

This choice being made, then, for any $\tilde{q}_0 = (q_0, t) \in E$, the set $\{(q, t) \mid q \in M\}$ is the image $s_{\tilde{q}_0}(M)$ of the canonical section $s_{\tilde{q}_0}$.

2.7. CANONICAL COMPLEX STRUCTURES

Let (E, Δ, g, X) be an isoperimetric structure, with $M = E/X$. There are two canonical complex structures, both denoted by J, on the fibers of TM and Δ. Both are defined by:

$$\mathrm{Vol}_g(u, v) = g(J(u), v), \tag{2.7}$$

where Vol_g is the volume (area) form associated with the metric g either on M or on Δ.

2.8. DECOMPOSITION OF TENSOR FIELDS

Let $\bigodot^k \Delta^*$ (resp. $\bigodot^k T^*M$) denote the tensor bundle of symmetric, k-covariant tensors over Δ (resp. TM). $\pi\colon E \to M = E/X$ is the canonical projection.

The structural group SO(2) of Δ and TM acts on the typical fibers (which are the same) of both bundles $\bigodot^k \Delta^*$ and $\bigodot^k T^*M$.

Here, the typical fibers $\bigodot^k \Delta^*(0)$, $\bigodot^k T^*M(0)$, as SO(2)-modules, have real decompositions:

$$\begin{aligned} \bigodot^k \Delta^*(0) &= \bigoplus_{j\in N} \Big(\bigodot^k \Delta^*(0) \Big)_j, \\ \bigodot^k T^*M(0) &= \bigoplus_{j\in N} \Big(\bigodot^k T^*M(0) \Big)_j, \end{aligned} \tag{2.8}$$

where the representation of SO(2) on the jth component of the right-hand side of (2.8) corresponds to the characters $e^{\varepsilon j\sqrt{-1}}$, $\varepsilon = +1, -1$. All nonzero j-components are 2-dimensional, except for $j = 0$ where they are 1-dimensional. The higher order term in the sum is $j = k$, and if k is odd (resp. even) all the even (resp. odd) components are zero.

Then, according to these decompositions of the typical fibers, we have decompositions of the bundles:

$$\begin{aligned} \bigodot^k \Delta^* &= \bigoplus_{j\in N} \Big(\bigodot^k \Delta^* \Big)_j, \\ \bigodot^k T^*M &= \bigoplus_{j\in N} \Big(\bigodot^k T^*M \Big)_j. \end{aligned} \tag{2.9}$$

If $p_0 \in M$, $q_0 \in \pi^{-1}(p_0)$, then, π induces a mapping $\pi_*\colon \bigodot^k T^*_{p_0}M \to \bigodot^k \Delta^*_{q_0}$, which is a linear isomorphism. The decompositions (2.9) of the bundles commute with this mapping π_*: if $T \in \bigodot^k T^*_{p_0}M$, $p_0 = \pi(q_0)$, $T = \sum T_j$, $T_j \in (\bigodot^k T^*_{p_0}M)_j$, then $\pi_*(T) = \sum \pi_*(T_j)$, $\pi_*(T_j) \in (\bigodot^k \Delta^*_{q_0})_j$.

This decomposition $T = \sum T_j$ of T is nothing but the real Fourier series of T, if T is identified to a function on the unit circle, via the identification of k-covariant symmetric tensors over Δ (resp. TM), with homogeneous polynomials of degree k on Δ^* (resp. T^*M).

All along the paper, this decomposition will be used extensively.

NOTATION. If k denotes the Gaussian curvature on M, then $\nabla^l k$ is a symmetric covariant tensor field of degree l over M. We will allow to write $\nabla^l_j k$ in place of $(\nabla^l k)_j$ in the previous decomposition.

2.9. NORMAL FORMS AND NORMAL COORDINATES

Let $I_{q_0} = (E, \Delta, g, X)_{q_0}$ denote a germ of isoperimetric structure at $q_0 \in E$. Set $M = E/X,\ p_0 = \pi(q_0)$.

For the germ at p_0 of Riemannian metric space $R_{p_0} = (M, g)_{p_0}$, we can consider the standard "normal coordinates" (x, y) from Riemannian geometry (see [12] for instance).

DEFINITION 2.3. The following coordinates (x, y, w) in a neighbourhood of q_0 are called *isoperimetric normal coordinates* at q_0:

(x, y) are normal Riemannian coordinates on the quotient M,
w is such that, if $q = \exp(tX)(s_{q_0}(p))$, then, $w(q) = t$.

Here, s_{q_0} is the canonical section defined in Section 2.5 above.

We prefer the letter w to the letter z for the third coordinate, keeping the z notation for $(x + iy)$, in accordance with the complex structure J over Δ defined in Section 2.7.

Consider the curve Γ: $]-\varepsilon, \varepsilon[\to E, \Gamma(t) = \exp(tX(q_0))$. In the (isoperimetric) normal coordinates (x, y, w), geodesics starting from $\Gamma(t)$, and satisfying the transversality conditions w.r.t. the curve $\Gamma(t)$ are straight lines through $\Gamma(t)$, contained in the planes $\{w = cst = t\}$. Similar coordinates have already been introduced in our previous papers [4, 9], where they have been called "(sub-Riemannian) normal coordinates". The main difference with these previous sub-Riemannian coordinates is that now, the vector field X writes

$$X = \frac{\partial}{\partial w}. \tag{2.10}$$

These coordinates *are uniquely defined* up to the action of SO(2) on Δ_{q_0} (or on $T_{p_0}M$).

Note 5. In these coordinates, $\Gamma(t) = (0, 0, t)$, and, for $s > 0$ small, the cylinders $C_s = \{(x, y, w) \mid x^2 + y^2 = s^2\}$ are just the set of points q such that $d(q, \{\Gamma(.)\}) = s$.

Following the same method as in our previous paper [4], one can easily prove the following theorem:

THEOREM 2.1. *In normal coordinates at q_0, there is a* (*unique up to the action of* SO(2) *on* Δ_{q_0}) *orthonormal frame field* (F, G) *for the sub-Riemannian metric, of the form*:

$$\begin{aligned} F &= \frac{\partial}{\partial x} - y\beta\left(x\frac{\partial}{\partial y} - y\frac{\partial}{\partial x}\right) + \frac{y}{2}\gamma\frac{\partial}{\partial w}, \\ G &= \frac{\partial}{\partial y} + x\beta\left(x\frac{\partial}{\partial y} - y\frac{\partial}{\partial x}\right) - \frac{x}{2}\gamma\frac{\partial}{\partial w}, \end{aligned} \tag{2.11}$$

where β, γ are smooth functions of x and y only.

The result of [4] in the general sub-Riemannian case is:

THEOREM 2.2. *There is a unique* (*unique up to the action of* SO(2) *on* Δ_{q_0}) *coordinate system, called the* sub-Riemannian normal coordinates*, and a unique* (*once the coordinates are chosen*) *orthonormal frame field* (F, G) *for the metric, of the form* (2.11)*, where the functions* β, γ *depend on* (x, y, w)*, but satisfy the boundary conditions*:

$$\begin{aligned} \gamma(0, 0, w) &= 1, \\ \beta(0, 0, w) &= \frac{\partial \gamma}{\partial x}(0, 0, w) = \frac{\partial \gamma}{\partial y}(0, 0, w) = 0. \end{aligned} \tag{2.12}$$

Note 6. (a) Theorem 2.2 is not obvious. See [4] for details and proof. In the isoperimetric case, it is much easier. Details of the proof are simple variations of the proof in [4].

(b) This normal form (2.11) (together with the boundary conditions 2.12), is invariant under the action of rotations on Δ_{q_0}: if $e^{J\theta_0}$ denotes the linear mapping $(x, y) \to (\cos(\theta_0)x - \sin(\theta_0)y, \sin(\theta_0)x + \cos(\theta_0)y)$ (see Section 2.7 above), then, setting $(x, y) = e^{J\theta_0}(\tilde{x}, \tilde{y})$, the orthonormal frame $(\tilde{F}, \tilde{G}) = e^{-J\theta_0}(F, G)$ is in normal form (2.11), with $\tilde{\beta} = \beta \circ e^{J\theta_0}$, $\tilde{\gamma} = \gamma \circ e^{J\theta_0}$.

(c) As a corollary, we find the classical normal form for 2-d Riemannian metrics: in normal coordinates with pole p_0, there is an orthonormal frame (unique up to rotations in $T_{p_0}M$), $(\bar{F}, \bar{G})$:

$$\begin{aligned} \bar{F} &= \frac{\partial}{\partial x} - y\beta\left(x\frac{\partial}{\partial y} - y\frac{\partial}{\partial x}\right), \\ \bar{G} &= \frac{\partial}{\partial y} + x\beta\left(x\frac{\partial}{\partial y} - y\frac{\partial}{\partial x}\right). \end{aligned} \tag{2.13}$$

This normal form is also invariant under the action of SO(2) in $T_{p_0}M$ (in the same sense as in (b) just above).

In the Dido case, the function γ can be computed in terms of the Riemannian structure of the quotient M, that is, in terms of β: using the fact that the characteristic vector field is $\nu = \partial/\partial w$ in our normal coordinates, we get:

THEOREM 2.3. *In the case of a Dido structure, the function* γ *in the isoperimetric normal form* (2.11) *is given by:*

$$\gamma(x, y) = \big(1 + (x^2 + y^2)\beta(x, y)\big) \int_0^1 \frac{2t\, dt}{1 + t^2(x^2 + y^2)\beta(tx, ty)}. \tag{2.14}$$

2.10. INVARIANTS

A normal coordinate system N_0 is chosen, together with a normal orthonormal frame (2.11). In these coordinates, the kth differentials $D^k\beta,\ D^k\gamma$ of these functions $\beta(x, y),\ \gamma(x, y)$ at the point p_0 ($x = y = 0$) in M are homogeneous polynomials of degree k in x, y. $D^k\beta, D^k\gamma$ define symmetric covariant tensors of degree k on $T_{p_0}M$, that we denote by β^k, γ^k. The point (b) in the Note 6 above shows that these tensors are independent of the choice of the normal orthonormal frame field: if (F, G) is changed for $(\tilde{F}, \tilde{G}) = \mathrm{e}^{-J\theta_0}(F, G)$, then the β^k, γ^k are changed for $\tilde{\beta}^k = \beta^k \circ \mathrm{e}^{J\theta_0},\ \tilde{\gamma}^k = \gamma^k \circ \mathrm{e}^{J\theta_0}$. It is also easy to check that, by construction, in the contact case, they do not depend on the orientation on M: if X is changed for $-X$, orientation on Δ is reversed and β and γ don't move. In the Dido case, if the orientation on M changes, ν is changed for $-\nu$.

COROLLARY 2.4. *The tensors β^k, γ^k on M are invariants of the isoperimetric structure. The β^k are invariants of the quotient Riemannian structure on M.*

The invariants β^l, that are the only ones in the Dido case, are related with the curvature on M as follows: let k denote the Gaussian curvature on M. Using the fact that (2.13) is an orthonormal frame on M in Riemannian normal coordinates with pole p_0, it is only a matter of simple computations to check that:

$$k(p_0) = 6\beta(p_0). \tag{2.15}$$

If ∇ denotes the covariant derivative on M,

$$\nabla k(p_0) = 12\beta^1(p_0). \tag{2.16}$$

$\nabla^2 k(p_0)$ is a 2-covariant symmetric tensor. It can be decomposed following Section 2.8:

$$\begin{aligned} \bigodot^2 T^*M &= \Big(\bigodot^2 T^*M\Big)_0 \oplus \Big(\bigodot^2 T^*M\Big)_2, \\ \nabla^2 k(p_0) &= \nabla_0^2 k(p_0) + \nabla_2^2 k(p_0). \end{aligned} \tag{2.17}$$

One has:

$$\begin{aligned} \nabla_0^2 k(p_0) &= 8\beta(p_0)\big((dx)^2 + (dy)^2\big), \\ \nabla_2^2 k(p_0) &= 20\beta_2^2(p_0), \end{aligned} \tag{2.18}$$

and:

$$\begin{aligned} \nabla^3 k(p_0) &= \nabla_1^3 k(p_0) + \nabla_3^3 k(p_0), \\ \nabla_3^3 k(p_0) &= 180\beta_3^3(p_0). \end{aligned} \tag{2.19}$$

In particular, for $j = 2, 3$, the "highest harmonics" in the decomposition of $\nabla^j k(p_0)$ and $\beta^j(p_0)$ *are nonzero constant multiples*: $\nabla_j^j k = \lambda_j\ \beta_j^j$ for some real

$\lambda_j \neq 0$. This follows from the fact that the curvature on $M = E/X$ is related with the function β in the normal forms (2.11), (2.13) by the following formula, with $z = x + iy$:

$$k(x, y) = \Big(6\beta + 10\beta^2|z|^2 + 2\beta^3|z|^4 + 2y\frac{\partial\beta}{\partial y}(3 + 2|z|^2\beta) + + 2x\frac{\partial\beta}{\partial x}\big(3 + 2|z|^2\beta\big) + x^2\frac{\partial^2\beta}{\partial x^2} + y^2\frac{\partial^2\beta}{\partial y^2} + 2xy\frac{\partial^2\beta}{\partial x\partial y}\Big)\Big/\big(1 + |z|^2\beta\big).$$

The formulas (2.16), (2.18) follow from this formula easily: since (x, y) are normal coordinates on M, covariant differentiation of any tensor field, at the pole $(x, y) = 0$ is just standard differentiation. (2.19) requires more computations.

2.11. SOLUTION OF THE ISOPERIMETRIC PROBLEM IN THE GENERAL CONTACT CASE

Let us consider the general case of an isoperimetric structure $I_{q_0} = (E, M, g, \pi, \Delta)_{q_0}$. Let α be the lift of the volume form over M, and let η be the curvature form of the connection, $\eta = \psi\alpha$. In the contact case, $\psi(q_0) \neq 0$.

We refer to our previous papers [2, 4, 9], about general contact sub-Riemannian structures. In these papers, two main invariants appear, denoted in [4, 9] by Q_2 and V_3.

In fact, Q_2 and V_3 are defined via the (nonisoperimetric) sub-Riemannian normal form of Theorem 2.2: In sub-Riemannian normal coordinates, using the decomposition of tensors introduced in the Section 2.8, $Q_2 = (Q)_2$, $V_3 = (V)_3$ where Q is the quadratic form $D^2_{x,y}\gamma(q_0)$, and $V = D^3_{x,y}\gamma(q_0)$.

Q_2 belongs to $(\bigodot^2 \Delta^*)_2$ and V_3 belongs to $(\bigodot^3 \Delta^*)_3$.

Set:

$$x_2 = \nabla^2 \log(\psi), \qquad x_3 = \nabla^3 \log(\psi), \tag{2.20}$$
$$x_2 \in \bigodot^2 \Delta^*, \qquad x_3 \in \bigodot^3 \Delta^*.$$

Denote by $x_{2,2}$ (resp. $x_{3,3}$) the component of x_2 (resp. x_3) in $(\bigodot^2 \Delta^*)_2$ (resp. $(\bigodot^3 \Delta^*)_3$). Computations show the following:

THEOREM 2.5 (Contact case). *Q_2 is a nonzero multiple of $x_{2,2,}$ and V_3 is a nonzero multiple of $x_{3,3}$.*

Hence, it is clear that, for an open dense set of contact isoperimetric sructures over a 2-d manifold M, $Q_2 \neq 0$ except at isolated points of M, and at these isolated points, $V_3 \neq 0$.

Therefore, *the study of generic isoperimetric problems is equivalent to the study of generic sub-Riemannian problems* (since most of the properties that we study are completely determined by Q_2 if nonzero, or V_3 if $Q_2 = 0$). In particular, the optimal synthesis for the isoperimetric problem follows.

The conjugate loci, cut loci, and sub-Riemannian spheres were described completely in our uppermentioned papers. These papers, in particular, solve the local isoperimetric problem. We refer to these papers for details.

An interesting remark is that, for these generic contact isoperimetric problems, the invariants β^k, that is, *the invariants of the Riemannian structure* over the quotient $M = E/X$, *play absolutely no role* in the shape of the local optimal synthesis, and have no influence on the singularities of spheres, on the shape of conjugate loci and cut loci.

2.12. DIDO CASE

In that case, the situation is completely different: ψ in (2.20) is a constant. Hence all covariant derivatives $\nabla^k \log(\psi)$ vanish identically. In particular, $Q_2 \equiv 0,\ V_3 \equiv 0$.

Therefore, all our previous results do not apply. *Our main purpose in the remaining of the paper is to study this "Dido case".*

2.13. WAVE FRONTS, SPHERES, CONJUGATE LOCI, CUT LOCI

The wave front of radius s is $W_s = \varepsilon(C_0, s)$, the sphere of radius s is the set $S_s = \{q \in E \mid d(q, q_0) = s\}$.

Standard arguments (of Filippov's type for instance) show that, for s small enough, if $d(q, q_0) = s$, there is at least a geodesic segment of length s joining q_0 to q. Hence $S_s \subset W_s$.

Also, any geodesic is optimal on small pieces of itself. For such a geodesic $\varepsilon(c, .), c \in C_0$, we define the conjugate-time (of the pole) $s_{\text{conj}}(c)$ (resp. the cut-time $s_{\text{cut}}(c)$) as the first time at which the geodesic ceases to be locally optimal – i.e., optimal among admissible curves having the same endpoints and lying in a certain C^0 neighbourhood of the geodesic segment (resp. globally optimal).

It is possible to check that $s_{\text{conj}}(c)$ is also the minimal strictly positive time at which the exponential mapping has not full rank.

The *conjugate locus* CL is the union $\bigcup_{c \in C_0} \varepsilon(c, s_{\text{conj}}(c))$, i.e. the set of (*first*) *singular values of the exponential mapping* ε. The cut locus $\text{Cut}\, L$ is the union $\bigcup_{c \in C_0} \varepsilon(c, s_{\text{cut}}(c))$.

By homogeneity of H, $\varepsilon(c, \lambda s) = \varepsilon(\lambda\, c, s)$. Hence, we can also consider ε as a map $\varepsilon\colon \bar{C}_0 \to E, \varepsilon(p) = \pi_E \circ \exp \mathbf{H}(p)$. In that case, let us denote it by $\bar{\varepsilon}$.

The conjugate locus is again part of the set of singular values of $\bar{\varepsilon}$. $\bar{C}_0$ is a Lagrangian submanifold of T^*E, which is mapped by $\exp \mathbf{H}(p)$ into another Lagrangian submanifold, hence $\bar{\varepsilon}$ is a Lagrangian mapping (in the sense of [6]), and the conjugate locus is part of the associated "caustic".

On the same way, $\varepsilon_s = \varepsilon(.,s)$: $C_0 \to E$ can be considered as a Legendre mapping (in the same sense), and its image is a standard "wave front".

Therefore, all the objects we will study (spheres, conjugate loci, cut loci) are, at the local level, elementary objects of the theory of Lagrangian and Legendrian singularities, in dimension 3. Of course, we will show nothing new at this level. What will be new is that, the elementary singularities appearing in our study consist of *nontrivial arrangements of classical* (*stable*) *Lagrangian and Legendrian singularities*. These collections of elementary stable singularities *are not organized in an arbitrary way*. In fact, we will study and classify the *global* (Lagrange and Legendre) "first" singularities of the mappings $\bar{\varepsilon}$ and ε_s. As the reader will see, they are very special.

Note 7. (a) We have already done this classification for generic sub-Riemannian metrics in our uppermentioned papers.

(b) We have shown (Section 2.11) above that the general case of generic isoperimetric structures falls down in this classification. We will do the same classification for Dido structures in the next sections.

(c) Let us recall what can occur for generic sub-Riemannian metrics, as elementary Lagrange and Legendre singularities. The following statements (c1), (c2) follow from a careful examination of our previous papers:

(c1) For caustics (conjugate loci), at generic points where $Q_2 \neq 0$, the only singularities are A_3 (cuspidal lines). At points where $Q_2 = 0$ but $V_3 \neq 0$, the same happens. Apparently, singularities of type A_4, D_4 don't appear generically. This is due to the fact (also true for Dido structures, as we shall see) that the exponential mapping ε is also the suspension of a stable (in the classical Thom–Mather sense) mapping between 2-dimensional manifolds. *Nevertheless, it is shown in the paper* [9] *that, in the transition between generic and nongeneric points, a singularity of type* A_4 (*swallow tail*) *appears*.

(c2) For wave fronts, the generic singularities that can appear are all the stable elementary Legendre singularities of dimension 3, that is A_2 (cuspidal lines) and A_3 (swallow tails) only.

2.14. REPARAMETRIZATION OF GEODESICS

$(x, y, w, \tilde{p}, \tilde{q}, r)$ are the isoperimetric normal coordinates and dual coordinates in T^*E. For $r \neq 0$, set:

$$p = \frac{\tilde{p}}{r}, \qquad q = \frac{\tilde{q}}{r}, \qquad \rho = \frac{1}{r}, \qquad t = rs \tag{2.21}$$

(t is the *new time*, s is the arclength).

In these coordinates, the cylinder $C_0 = \{p = \rho\cos(\varphi), q = \rho\sin(\varphi)\}$, and ε is a mapping of the variables (ρ, φ, t), *which is smooth* even at $\rho = 0$. We denote it again by $\varepsilon(\rho, \varphi, t)$. Setting $z = (x, y)$, ε_z denotes the two first components of ε,

and ε_w denotes the third one. $\varepsilon_z, \varepsilon_w$ have expansions in terms of ρ, at $\rho = 0$, of the form:

$$\begin{aligned} \varepsilon_z &= \rho\varepsilon_1^z(t,\varphi) + \rho^3\varepsilon_3^z(t,\varphi) + \cdots + \rho^n\varepsilon_n^z(t,\varphi) + \mathrm{o}(\rho^{n+1}) \\ &= \tilde{\varepsilon}_n^z + \mathrm{o}(\rho^{n+1}) \end{aligned} \tag{2.22}$$

(note the very important point that the *term of order* 2 *is missing*),

$$\begin{aligned} \varepsilon_w &= \rho^2\varepsilon_2^w(t,\varphi) + \rho^4\varepsilon_4^w(t,\varphi) + \cdots + \rho^n\varepsilon_n^w(t,\varphi) + \mathrm{o}(\rho^{n+1}) \\ &= \tilde{\varepsilon}_n^w + \mathrm{o}(\rho^{n+1}). \end{aligned} \tag{2.23}$$

Let us set also $\varepsilon_1 = (\rho\varepsilon_1^z(t,\varphi), \rho^2\varepsilon_2^w(t,\varphi))$, $\bar{\varepsilon}_n = (\tilde{\varepsilon}_n^z(t,\varphi), \tilde{\varepsilon}_{n+1}^w(t,\varphi))$.

Note 8. (a) $\bar{\varepsilon}_1 = \varepsilon_1$ is just the exponential mapping of the "Heisenberg" right-invariant metric, which is the basic model. Everything will be computed by using formulas (2.22), (2.23), as a perturbation of this basic (and totally degenerate) exponential mapping. Half a wave front of this Heisenberg metric is shown on the Figure 2 (the part $w > 0$).

(b) These formulas (2.22), (2.23) hold in the Dido case, in the isoperimetric normal coordinates, and in other cases in the sub-Riemannian normal coordinates. In particular, they don't hold in the generic isoperimetric case, for isoperimetric normal coordinates. But, in that case, we can forget with the isoperimetric character, as we said in the Section 2.11.

ε_1 can be computed easily:

$$\begin{aligned} \varepsilon_1(\rho,\varphi,t) &= (\rho\varepsilon_1^z(t,\varphi), \rho^2\varepsilon_2^w(t,\varphi)), \\ \varepsilon_1^z(t,\varphi) &= (2\cos(\varphi - t/2)\sin(t/2), 2\sin(\varphi - t/2)\sin(t/2)), \\ \varepsilon_2^w(t,\varphi) &= (t - \sin(t))/2. \end{aligned} \tag{2.24}$$

We will show in Section 3.1 how to compute the other terms that we need in the formulas (2.22), (2.23). Depending on the context, we will need to compute $\bar{\varepsilon}_n$ for $n = 5$ or $n = 6$.

2.15. SUFFICIENT JETS FOR THE EXPONENTIAL MAPPING

There are three ways to consider the exponential mapping: if s denotes the arclength parameter, then, (1) we can consider $\bar{\varepsilon}$ as a Lagrangian mapping, or (2) we can consider, for s fixed, ε_s as a Legendrian mapping. As we shall see in Section 3.2, it will be also possible and convenient (3) to consider ε as the suspension of an ordinary smooth mapping between 2-dimensional manifolds.

Similarly to the case of generic sub-Riemannian problems, or to the case of generic isoperimetric problems, the exponential mapping will be *stable* as an ordinary mapping (in restriction to a neighbourhood of its first singular set). All singularities that will appear will just be suspensions of stable singularities of

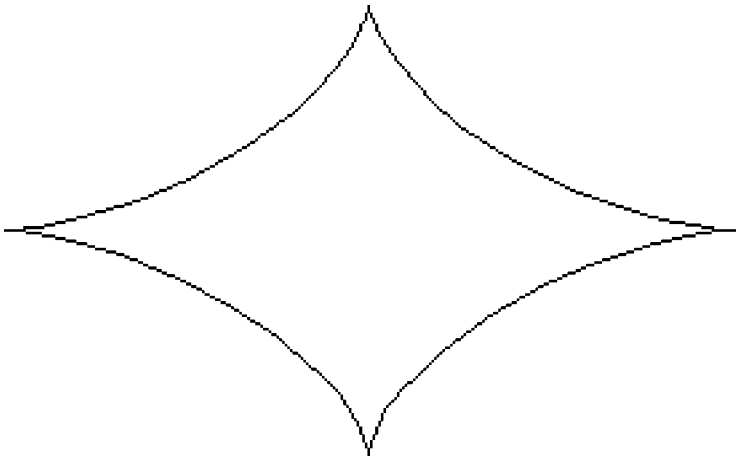

Figure 3. Conjugate locus, nondegenerate case.

ordinary mappings between 2-d manifolds (3), stable singularities of Lagrangian mappings (1), or stable singularities of Legendrian mappings (2).

As a standard (suspended) map, the exponential mapping will have "sufficient jets" with respect to ρ (at the local level around the pole q_0, ρ has to be small; φ is any, and t has to be close to the Heisenberg conjugate time $t_H = 2\pi$).

By a "sufficient jet", we mean always that, in restriction to certain neighbourhoods of the singular sets at the source of both the mapping and the jet, the mapping and the jet are left–right equivalent. Moreover the equivalence is such that the diffeomorphisms at the image preserve the w coordinate (which is intrinsic, the germ of Dido structure being given).

Also, the sufficient jet will be determined by certain finite jets of the sub-Riemannian structure on E, or, in the Dido case, by certain jets of the Riemannian structure on $M = E/X$.

Due to a certain *asymptotic symmetry* that will appear, it is very complicated to compute "global" sufficient jets of ε in all generic cases (this has been done for generic sub-Riemannian metrics in the paper [4]). We will say a few words about that in Section 3.4 for the Dido case. But, we will show that, to describe the (global) singularities of the spheres, *local stability only* of ε along its singular set is sufficient.

Precisely, we will have to consider two situations:

(a) points q_0 of E such that, if $p_0 = \pi_X(q_0)$, $\nabla_2^2 k(p_0) \neq 0$. In that case, $\bar{\varepsilon}_5$ will be a *globally* sufficient jet for ε, with respect to left-right equivalence, on a neighbourhood of the first singular set.

(b) points q_0 of E such that $\nabla_2^2 k(p_0) = 0$ but $\nabla_3^3 k(p_0) \neq 0$. In that case, we need the jet $\bar{\varepsilon}_6$. Along its singular set, ε is only *locally* equivalent to this jet.

3. The Dido Case

3.1. COMPUTATION OF THE EXPONENTIAL MAPPING

As we said, we will have to compute all terms in formulas (2.22), (2.23), for $n = 5$ if $\nabla_2^2 k(p_0) \neq 0$, and for $n = 6$ if $\nabla_2^2 k(p_0) = 0$.

To compute these terms, one can proceed as follows:

Set $\varsigma = (x, y, p, q)$. Then, our geodesics have the expansion:

$$\begin{aligned} \varsigma(\rho, \varphi, t) &= \varsigma^n(\rho, \varphi, t) + \mathrm{o}(\rho^{n+1}), \\ \varsigma^n(\rho, \varphi, t) &= \rho\varsigma_1(\varphi, t) + \rho^3\varsigma_3(\varphi, t) + \cdots + \rho^n\varsigma_n(\varphi, t), \end{aligned} \tag{3.1}$$

$\varsigma_1(\rho, \varphi, t)$ is the "Heisenberg term", the two first components of which are given in (2.24). Let $\mathbf{B}$ denote the $(x, y, \tilde{p}, \tilde{q})$ components of our vector field $\mathbf{H}$, in which moreover we set $r = 1$, $\tilde{p} = p$, $\tilde{q} = q$. Let $\mathbf{B}_n$ denote the nth jet of $\mathbf{B}$ with respect to $\varsigma = (x, y, p, q)$. Then, we can compute $\varsigma_n(\varphi, t)$ by induction, because:

$$\begin{aligned} \varsigma^{n+1} &= \rho\varsigma_1(\varphi, t) + \int_0^t \mathrm{e}^{A(t-s)}(\mathbf{B}_{n+1} - \mathbf{B}_1)(\varsigma^n(\rho, \varphi, s))\,\mathrm{d}s + \\ &\quad + \mathrm{o}(\rho^{n+2}), \end{aligned} \tag{3.2}$$

where $A(x, y, p, q) = \mathbf{B}_1(x, y, p, q)$ is the Heisenberg linear operator with matrix:

$$A = \begin{pmatrix} 0 & 1/2 & 1 & 0 \\ -1/2 & 0 & 0 & 1 \\ -1/4 & 0 & 0 & 1/2 \\ 0 & -1/4 & -1/2 & 0 \end{pmatrix}.$$

After this the components of ε_i^w are obtained by simple integration because our Hamiltonian H does not depend on the w variable:

$$\frac{\mathrm{d}w}{\mathrm{d}t} = \frac{\partial H}{\partial r}(\varsigma)_{|r=1}. \tag{3.3}$$

These computations are rather long. We did similar computations by the hand in our previous papers, for generic sub-Riemannian metrics. Here, we used a Formal program (using Mathematica) to compute these terms. This program is given in our Appendix A1. It is just based upon the formula (3.2). We show here the expressions of ε_3^z and ε_4^w. The other expressions are too long.

In the following formulas, $\alpha_0 = 1/6\, k(p_0)$.

$$\begin{aligned} \varepsilon_3^z &= \alpha_0/2(6t\cos(\varphi - t) - 6\sin(\varphi) + 2\sin(\varphi - 2t) + \\ &\quad + 3\sin(\varphi - t) + \sin(\varphi + t), \\ &\quad 6t\sin(\varphi - t) + 6\cos(\varphi) - 2\cos(\varphi - 2t) - \\ &\quad - 3\cos(\varphi - t) - \cos(\varphi + t)), \\ \varepsilon_4^w &= 3\alpha_0/8(-2t - 4t\cos(t) + 4\sin(t) + \sin(2t)). \end{aligned} \tag{3.4}$$

3.2. THE EXPONENTIAL MAPPING AS A SUSPENSION

It is possible, and very convenient for our purposes to chose coordinates at the source of the exponential mapping so that it is in suspended form. A simple computation shows that the conjugate time for the Heisenberg approximation $\bar{\varepsilon}_1(\rho, \varphi, t)$, is $t_H = 2\pi$. Hence all the phenomena of importance occur for t close to 2π. We will set, for $w > 0$ and $\rho > 0$:

$$h = \sqrt{w/\pi}, \qquad \sigma = (s - 2\pi h)/h, \tag{3.5}$$

and we will use the coordinates (x, y, h) at the image and (φ, σ, h) at the source.

One can check that these coordinate changes are valid, in a certain neighbourhood of $\{t = s/\rho = 2\pi\}$ at the source (just using the expression (2.24) of ε_2^w).

Note 9. The case $w < 0,\ \rho < 0$ is absolutely similar, and leads to completely parallel results. Also, the results for $w < 0$ can be obtained from results for $w > 0$ just by reversing the orientation a posteriori. *From now on, we will consider the case $w > 0$ only.*

Note 10. In our previous papers, we used the coordinate systems (φ, t, h) or (φ, t, ρ) at the source. As we shall see, this new couple of coordinate systems (φ, σ, h) and (x, y, h) is very convenient for the computation the cut locus.

Also, the next lemma shows that it is very convenient for the computation of the conjugate locus.

LEMMA 3.1. *In the coordinates (x, y, h) at the image, and (φ, σ, h) at the source, the following properties hold*:

(i) *the conjugate time is given by the equation $\partial\varepsilon/\partial\varphi = 0$,*
(ii) *the conjugate time $\sigma_{\text{conj}}(\varphi, h)$, for h constant, is a function of φ having its extrema at the position φ of cusp points of the conjugate locus.*

Proof. For the same reason as in our previous papers, the conjugate time is a smooth function $\sigma_{\text{conj}}(\varphi, h)$. We consider the exponential mapping in suspended form, denoted here by $\hat{\varepsilon}(\varphi, h, \sigma) = (\hat{z}(\varphi, h, \sigma), h)$ for convenience. The regular exponential mapping, with coordinates (φ, ρ, s) at the source and (x, y, h) at the image is denoted by $\varepsilon(\varphi, \rho, s)$ (remember that $h = \sqrt{\frac{w}{\pi}}$ and $\sigma = (s - 2\pi h)/h$). The coordinate change at the source is $F(\varphi, h, \sigma) = (\varphi, \rho(\varphi, h, (\sigma + 2\pi)h),\ (\sigma + 2\pi)h)$. We fix h and we assume that φ_0 is a cusp point of the conjugate locus at h. The conjugate time function is denoted by $\sigma^h_{\text{conj}}(\varphi)$. The Liouville form restricted to $H_{1/2}$ is a contact form which gives to $H_{1/2}$ its contact structure. It is denoted by ω.

Let π_E: $T^*E \to E$. If $V \in T_{\varepsilon(\varphi,\rho,s)}E$, $V = T\pi_E(W)$, $W \in T_{\exp s\mathbf{H}(\varphi,\rho)}T^*E$, then $\omega(W) = \exp s\mathbf{H}(\varphi, \rho)(V)$. If W is tangent to a Legendre submanifold of $H_{1/2}$, then $\omega(W) = \exp s\mathbf{H}(\varphi, \rho)(V) = 0$. Let us write also ω for $\exp s\mathbf{H}(\varphi, \rho)$.

So that ω evaluates on $V = \frac{\partial}{\partial\varphi}(\hat{\varepsilon}(\varphi, h, \sigma))$ and $V' = \frac{\partial}{\partial\sigma}(\hat{\varepsilon}(\varphi, h, \sigma))$. But, $V = \frac{\partial\varepsilon}{\partial\varphi} \circ F + \frac{\partial\varepsilon}{\partial\rho} \circ F \frac{\partial}{\partial\varphi}(\rho(\varphi, h, (\sigma + 2\pi)h))$, and ω vanishes on $\frac{\partial\varepsilon}{\partial\varphi}$, $\frac{\partial\varepsilon}{\partial\rho}$ because they are projections on TE of tangent vectors to a Legendre manifold. $\omega(V) = 0$. Also, $V' = \frac{\partial\varepsilon}{\partial s} \circ F\, h + \frac{\partial\varepsilon}{\partial\rho} \circ F \frac{\partial}{\partial\sigma}(\rho(\varphi, h, (\sigma + 2\pi)h))$. Again, ω vanishes on $\frac{\partial\varepsilon}{\partial\rho}$, and $\omega(\frac{\partial\varepsilon}{\partial s}) = 1$ (the reason of this last property is that the Hamiltonian is quadratic in the adjoint variables: $\omega(\mathbf{H}) = 2H$). Therefore, $\omega(V') = h$.

If φ_0 is a cusp point, $\frac{\partial}{\partial\varphi}(\hat{\varepsilon}(\varphi_0, h, \sigma^h_{\text{conj}}(\varphi_0))) = 0$. Hence,

$$0 = \omega\left(\frac{\partial\hat{\varepsilon}}{\partial\varphi}\right) + \omega\left(\frac{\partial\hat{\varepsilon}}{\partial\sigma}\right)\frac{\partial\sigma^h_{\text{conj}}}{\partial\varphi}(\varphi_0).$$

Therefore, $\frac{\partial\sigma^h_{\text{conj}}}{\partial\varphi}(\varphi_0) = 0$.

Conversely, if $\frac{\partial\sigma^h_{\text{conj}}}{\partial\varphi}(\varphi_0) = 0$, then $\frac{\partial}{\partial\varphi}(\hat{\varepsilon}(\varphi_0, h, \sigma^h_{\text{conj}}(\varphi_0))) = 0$ by (i). This shows (ii).

To show (i), let us first write $\omega = \tilde{\omega}\,\mathrm{d}z + \omega_h\,\mathrm{d}h = \tilde{\omega}_1\,\mathrm{d}x + \tilde{\omega}_2\,\mathrm{d}y + \omega_h\,\mathrm{d}h$. $\tilde{\omega}$ is nonzero because $\omega(V') = h$. ω_h is nonzero because r is constant along geodesics (it is easy to see that for $r = 0$, there is no conjugate point close to the pole q_0). Set $\alpha = -\tilde{\omega}_2\,\mathrm{d}x + \tilde{\omega}_1\,\mathrm{d}y$. (φ, h, σ) belongs to the singular set of $\hat{\varepsilon}$ iff $(\omega \wedge \alpha \wedge \mathrm{d}h)(\frac{\partial\hat{\varepsilon}}{\partial\varphi}, \frac{\partial\hat{\varepsilon}}{\partial\sigma}, \frac{\partial\hat{\varepsilon}}{\partial h}) = 0$, or $(\tilde{\omega} \wedge \alpha)(\frac{\partial\hat{z}}{\partial\varphi}, \frac{\partial\hat{z}}{\partial\sigma}) = 0$, or equivalently $\tilde{\omega}(\frac{\partial\hat{z}}{\partial\varphi})\alpha(\frac{\partial\hat{z}}{\partial\sigma}) - \tilde{\omega}(\frac{\partial\hat{z}}{\partial\sigma})\alpha(\frac{\partial\hat{z}}{\partial\varphi}) = 0$, but $\tilde{\omega}(\frac{\partial\hat{z}}{\partial\varphi}) = 0$, $\tilde{\omega}(\frac{\partial\hat{z}}{\partial\sigma}) = h$. Hence, $\alpha(\frac{\partial\hat{z}}{\partial\varphi}) = 0$ and $\tilde{\omega}(\frac{\partial\hat{z}}{\partial\varphi}) = 0$. $\frac{\partial\hat{\varepsilon}}{\partial\varphi} = 0$. □

Remark 3.1. It follows from the asymptotics given in the next sections that, for h sufficiently small:

(1) If φ_0 is such that $\frac{\partial\sigma^h_{\text{conj}}}{\partial\varphi}(\varphi_0) = 0$, then $\frac{\partial^2\sigma^h_{\text{conj}}}{\partial\varphi^2}(\varphi_0) \neq 0$. This shows that local extrema of the conjugate time are characterized by the condition $\frac{\partial\sigma^h_{\text{conj}}}{\partial\varphi}(\varphi_0) = 0$.

(2) If φ_0 is such that $\frac{\partial}{\partial\varphi}(\hat{\varepsilon}(\varphi_0, h, \sigma^h_{\text{conj}}(\varphi_0))) = 0$, then $\frac{\partial^2}{\partial\varphi^2}(\hat{\varepsilon}(\varphi_0, h, \sigma^h_{\text{conj}}(\varphi_0))) \neq 0$. This shows that simple cusp points of the conjugate locus are characterized by the condition $\frac{\partial}{\partial\varphi}(\hat{\varepsilon}(\varphi_0, h, \sigma^h_{\text{conj}}(\varphi_0))) = 0$.

These two facts are implicitly used in the proof above.

From now on in this section, coordinates at the image and at the source of the exponential mapping will be the suspended coordinates (x, y, h) and (φ, σ, h).

It is just a matter of tedious but trivial computations (done in the Appendices 2–3) to get the expression of ε in these coordinates, from its expression computed in Section 3.1.

We use the following notations: $\alpha_0 = 1/6\, k(p_0)$, and, with the notations of our Section 2.8,

$$\beta_1(p_0) = r_1 \cos(t_1)\,\mathrm{d}x - r_1 \sin(t_1)\,\mathrm{d}y = 1/12 \bigtriangledown k(p_0), \tag{3.6}$$
$$\beta_2^2 = r_2 R_e(\mathrm{e}^{it_2}(\mathrm{d}x + i\,\mathrm{d}y)^2),\ \beta_0^2 = \tau_2(\mathrm{d}x^2 + \mathrm{d}y^2),$$

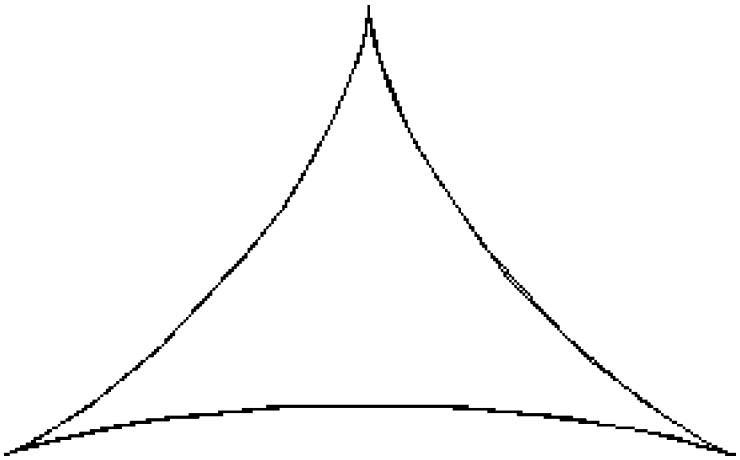

Figure 4. Conjugate locus, degenerate case.

$$\beta_1^3 = (r_{31}\cos(t_{31})\,\mathrm{d}x - r_{31}\sin(t_{31})\,\mathrm{d}y) \odot (\mathrm{d}x^2 + \mathrm{d}y^2),$$
$$\beta_3^3 = r_{32}R_e(\mathrm{e}^{it_{32}}(\mathrm{d}x + i\,\mathrm{d}y)^3).$$

By Section 2.10, $\nabla_2^2 k = 0$ iff $r_2 = 0$, $\nabla_3^3 k = 0$ iff $r_{32} = 0$.
Setting $\varepsilon(\varphi, \sigma, h) = (\varepsilon_s(\varphi, \sigma), h) = (x_s(\varphi, \sigma), y_s(\varphi, \sigma), h)$, we get:
(1) if $\nabla_2^2 k(p_0) \neq 0$:

$$z_s(\varphi, \sigma, h) = (x_s(\varphi, \sigma, h), y_s(\varphi, \sigma, h)) = z_s^5(\varphi, \sigma, h) + o^6(h, \sigma),$$
$$\begin{aligned} x_s(\varphi, \sigma, h) &= h/48((72\alpha_0 h^2\pi - 197(\alpha_0)^2 h^4\pi - 360h^4\pi r_2 + 48\sigma + 320h^4\pi\tau_2) \times \\ &\quad \times \cos(\varphi) + 6(20h^4\pi r_2\cos(3\varphi) + 9(\alpha_0)^2 h^4\pi^2\sin(\varphi) + \\ &\quad + 12\alpha_0 h^2\pi\sigma\sin(\varphi) + 4\sigma^2\sin(\varphi) + 24h^3\pi r_1\sin(t_1))) + o^6(h, \sigma), \end{aligned} \tag{3.7}$$

$$\begin{aligned} y_s(\varphi, \sigma, h) &= h/48((72\alpha_0 h^2\pi - 197(\alpha_0)^2 h^4\pi + 480h^4\pi r_2 + 48\sigma + 320h^4\pi\tau_2) \times \\ &\quad \times \sin(\varphi) - 6(3\alpha_0 h^2\pi + 2\sigma)^2\cos(\varphi) + 144h^3\pi r_1\cos(t_1) + \\ &\quad + 240h^4\pi r_2\cos(2\varphi)\sin(\varphi)) + o^6(h, \sigma), \end{aligned} \tag{3.8}$$

in which $o^6(h, \sigma)$ has order 6 in h, σ, *when* h *and* σ *have respectively weights* 1 *and* 2.

(2) If $\nabla_2^2 k = 0$ (or equivalently $r_2 = 0$), we find the following more complicated expressions, at the next order 6 in h, σ, that are computed in the program of our Appendix 3:

$$\bar{z}_s(\varphi, \sigma, h) = (\bar{x}_s(\varphi, \sigma, h), \bar{y}_s(\varphi, \sigma, h)) = \bar{z}_s^6(\varphi, \sigma, h) + o^7(h, \sigma),$$
$$\begin{aligned} \bar{x}_s(\varphi, \sigma, h) &= h/48(72\alpha_0 h^2\pi - 197(\alpha_0)^2 h^4\pi + 48\sigma + 320h^4\pi\tau_2)\cos(\varphi) + \end{aligned}$$

$$+ 6(3h^3\pi r_1(3\alpha_0 h^2\pi + 2\sigma)\cos(t_1) + (9\alpha_0 h^5\pi^2 r_1 + 6h^3\pi r_1\sigma) \times$$
$$\times \cos(2\varphi + t_1) + 9(\alpha_0)^2 h^4\pi^2 \sin(\varphi) + 12\alpha_0 h^2\pi\sigma \sin(\varphi) + 4\sigma^2 \sin(\varphi) -$$
$$- 120h^5\pi r_{32} \sin(2\varphi) + 60h^5\pi r_{32} \sin(4\varphi) + (24h^3 - 124\alpha_0 h^5)\pi r_1 \times$$
$$\times \sin(t_1) - 100h^5\pi r_{31} \sin(t_{31}))) + o^7(h, \sigma), \tag{3.9}$$

$$\bar{y}_s(\varphi, \sigma, h)$$
$$= -h/48(6(3\alpha_0 h^2\pi + 2\sigma)^2 \cos(\varphi) + 360h^5\pi r_{32}(2\cos(2\varphi) + \cos(4\varphi)) -$$
$$- 144h^3\pi r_1 \cos(t_1) + 744\alpha_0 h^5\pi r1 \cos(t_1) - 600h^5\pi r_{31} \cos(t_{31}) +$$
$$+ \alpha_0 h^2\pi \sin(\varphi)(197h^2\alpha_0 - 72) - 48\sigma \sin(\varphi) - 320h^4\pi\tau_2 \sin(\varphi) +$$
$$+ 36h^3\pi r_1\sigma \sin(t_1) + 54\alpha_0 h^5\pi^2 r_1(\sin(t_1) - \sin(2\varphi + t_1)) -$$
$$- 36h^3\pi r_1\sigma \sin(2\varphi + t_1)) + o^7(h, \sigma). \tag{3.10}$$

3.3. CONJUGATE LOCI AND LEFT-RIGHT STABILITY OF THE EXPONENTIAL MAPPING

To compute the conjugate time, we use the expressions of the exponential mapping in suspended form that we just computed. We have just to apply our Lemma 3.1 to $z_s(\varphi, \sigma, h) = (x_s(\varphi, \sigma, h), y_s(\varphi, \sigma, h))$. The computation, based upon the preceding formulas gives:

(1) case $\nabla_2^2 k \neq 0$ ($r_2 \neq 0$):

$$0 = -3/2\alpha_0 h^2\pi + 197/48(\alpha_0)^2 h^4\pi - \sigma -$$
$$- 20/3h^4\pi\tau_2 - 15h^4\pi r_2 \cos(2\varphi) + o^5(h, \sigma) \tag{3.11}$$

(for the sake of simplicity, *in that case we set* $t_2 = 0$),

(2) case $r_2 = 0$:

$$0 = -3/2\alpha_0 h^2\pi + 197/48(\alpha_0)^2 h^4\pi - \sigma - 20/3h^4\pi\tau_2 -$$
$$- 3/2h^3\pi r_1(3\alpha_0 h^2\pi + 2\sigma)\cos(\varphi + t_1) - 60h^5\pi r_{32} \sin(3\varphi) +$$
$$+ o^6(h, \sigma) \tag{3.12}$$

(*in that case, we set* $t_{32} = 0$).

We obtain the expansion of the conjugate time in both cases:

$r_2 \neq 0$:

$$\sigma_{\text{conj}}(\varphi, h) = h^2\pi/48(-72\alpha_0 + 197(\alpha_0)^2 h^2 - 320h^2\tau_2 -$$
$$- 720h^2 r_2 \cos(2\varphi)) + o^5(h), \tag{3.13}$$

$r_2 = 0$:

$$\bar{\sigma}_{\text{conj}}(\varphi, h) = -h^2\pi/48(72\alpha_0 - 197(\alpha_0)^2 h^2 + 320h^2\tau_2 +$$
$$+ 2880h^3 r_{32} \sin(3\varphi)) + o^6(h). \tag{3.14}$$

Just replacing in the expressions (3.7), (3.8), (3.9), (3.10), gives the asymptotics of the conjugate locus in suspended coordinates:

$r_2 \neq 0$:

$$\begin{aligned} z_{\text{conj}}(\varphi, h) &= z^5_{\text{conj}}(\varphi, h) + o^6(h) \\ &= h^4\pi(3r_1 \sin(t_1) - 15hr_2 \cos(\varphi) - 5h.r_2 \cos(3\varphi), \\ &\quad 3r_1 \cos(t_1) + 20hr_2 \sin(\varphi)^3) + o^6(h). \end{aligned} \tag{3.15}$$

$r_2 = 0$:

$$\begin{aligned} \bar{z}_{\text{conj}}(\varphi, h) &= z^6_{\text{conj}}(\varphi, h) + o^7(h) \\ &= -h^4\pi/2(-6r_1 \sin(t_1) + \\ &\quad + h^2(31\alpha_0 r_1 \sin(t_1) + 25r_{31} \sin(t_{31})) + \\ &\quad + 45h^2 r_{32}(2\sin(2\varphi) + \sin(4\varphi)), \\ &\quad - 6r_1 \cos(t_1) - h^2(25r_{31} \cos(t_{31}) - \\ &\quad - 31\alpha_0 r_1 \cos(t_1)) + 45h^2 r_{32}(2\cos(2\varphi) - \cos(4\varphi))) + \\ &\quad + o^7(h). \end{aligned} \tag{3.16, 3.17}$$

The two Figures 3, 4, show the shapes of these conjugate loci (cutting by $h = cst$).

The following theorem is not hard to prove:

THEOREM 3.2. *On a* 2-d *dimensional manifold M, there is an open-dense set* (*in the Whitney topology*) *of Riemannian metrics such that:*

(a) *on an open dense subset of M which is the complement of a discrete subset, $r_2 \neq 0$* (*equivalently, $\nabla^2_2 k \neq 0$*),

(b) *at the remaining isolated points, $r_{32} \neq 0$* (*equivalently $\nabla^3_3 k \neq 0$*).

DEFINITION 3.1. We call these germs of generic Riemannian metrics (or Dido structures) at points of M, nondegenerate in the case (a) and degenerate in the case (b).

Remark 3.2. $\nabla^2_2 k$, $\nabla^3_3 k$ take values in 2-dimensional spaces (spaces of nontrivial real irreducible representations of SO(2)). It is why the condition $\nabla^2_2 k = 0$ has codimension 2 and gives rise to isolated points.

Note 11. (a) As we see, sections by $h = cst$ of the conjugate locus in the nondegenerate case are still astroids (asymptotically). They are smaller than in the nondegenerate general sub-Riemannian case: in that case, the size is of order h^3, and here they have order h^5. Moreover now, these astroids are shifted by a term which is normal to the gradient of the curvature, the length of this term having order h^4.

(b) In the degenerate case, the conjugate locus has size h^6 in place of h^4 in the case of general sub-Riemannian metrics. For this 6th approximation, sections

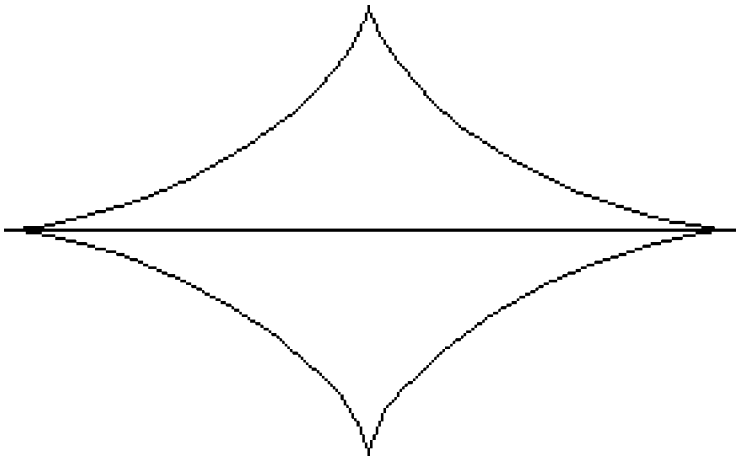

Figure 5. Cut locus, nondegenerate case.

by $h = cst$ are still *double* closed curves with 3 cusp points (6, in fact). This *asymptotic symmetry of π is very important*, as in the general sub-Riemannian case.

(c) These estimates use the expansions $\bar{\varepsilon}_5$, $\bar{\varepsilon}_6$ respectively, that is the 6th and 7th jets of the exponential mapping with respect to ρ (this is due to the presence of $\tilde{\varepsilon}^w_{n+1} in$ the definition of $\bar{\varepsilon}_n$). These jets are determined respectively by the 2nd and 3rd jets of the curvature at the pole p_0 in M.

Let us now examine the finite determinacy of ε in the sense of left-right equivalence. The results will be also perfectly parallel to those of the general case.

It follows from the computations above that the two mappings $z^5_s(\varphi, \sigma, h)$ and $\bar{z}^6_s(\varphi, \sigma, h)$ have the following properties for h fixed, small enough, as mappings between two dimensional manifolds, $(\varphi, \sigma) \to (x, y)$:

(a) their (first) singular locus at the source, are smooth curves,

(b) the image curves by the mappings present only fold points and cusp points (for definition, see Whitney [18], or Mather [14]),

(c) *for* $z^5_s(\varphi, \sigma, h)$, the restriction to this smooth curve S_h of the mapping is injective and proper. For $\bar{z}^6_s(\varphi, \sigma, h)$, this is true locally only.

We call such maps "Whitney maps". A Whitney map is stable (for left-right equivalence).

If S denotes the (first) singular set of the exponential mapping ε, and $\bar{S}_5$ (resp. $\bar{S}_6$) denote the singular set of the $\rho-$jet $\bar{\varepsilon}_5$ (resp. $\bar{\varepsilon}_6$), then, using this stability property and exactly the same arguments as in our paper [9], it is easy to show that ε and $\bar{\varepsilon}_5$ (resp. $\bar{\varepsilon}_6$), are left-right equivalent when restricted to certain neighbourhoods of S and $\bar{S}_5$ (resp. $\bar{S}_6$). This last statement is true globally on a neighbourhood of the singular set S in the nondegenerate case and locally only along S in the degenerate case. The diffeomorphisms at the image can be chosen w-preserving.

THEOREM 3.3. *For $h > 0$, small enough: the suspended exponential mapping $\varepsilon(\varphi, \sigma, h)$ for a generic Dido structure is left-right equivalent via h-preserving*

diffeomorphisms (*in restriction to a certain open neighbourhood of its first singular set S at the source*) *to its* 5*th jet* (*resp.* 6*th*) *w.r.t. h at the points q_0 where the structure is nondegenerate* (*resp. degenerate*). *This statement is true globally along S for nondegenerate points q_0, and locally only for degenerate ones.*

Note 12. In [4], we examined the question of global stability of ε in a neighbourhood of S in the degenerate case, for general sub-Riemannian metrics. It is an interesting problem in itself, but it is rather difficult. We gave a complete generic classification, in which appear 7 different types of degeneracy, and we computed all sufficient jets, that can have high order. However, it appears that this classification has absolutely no influence on the optimal synthesis: *The optimal parts of the wave fronts* (i.e., the spheres), *do not depend on this classification*. Differences can be seen only at the level of nonoptimal parts of wave fronts (although for t close to $t_H = 2\pi$).

Here, the situation will be the same: *this question of finding all globally sufficient jets is of no importance for the optimal synthesis in the Dido problem*. Nevertheless, all detailed computations have been done for the Dido problem in [7].

Due to the extra symmetry, there are several differences with the nonisoperimetric sub-Riemannian case, even for general isoperimetric problems. In the next section, we state the main result, in Dido case, without the proof which is very similar to that of [4].

3.4. SYMBOLS FOR CONJUGATE LOCI

For generic Riemannian metrics in the degenerate case, the asymptotic symmetry, which appears at the level of the approximation $\bar{\varepsilon}_4$, is broken at the level of higher order jets.

That is, considering higher order jets, when cut by $h = cst$, germs of conjugate loci at the pole q_0 are closed curves in general position, presenting 6 cusp points, and transversal self-intersections. These curves are typically denoted by Γ_h.

This happens at the level of the approximation $\bar{\varepsilon}_7$ for the highest codimension case.

In the Dido case, the asymptotic symmetry, which appears at the level of the jet $\bar{\varepsilon}_6$, is broken at the level of the approximation $\bar{\varepsilon}_8$ (which is determined by the 5th jet of the curvature at the pole p_0 of M). In that case the curves Γ_h, sections of the conjugate locus by $h = cst$, are also closed curves in general position, with 6 cusp points and transversal self-intersections.

As in the general case, let us define the *symbol* of a conjugate locus as follows: We select any cusp point on Γ_h and any orientation on Δ. We count the number of self intersections of Γ_h between the ith and $(i+1)$th cusp point, and divide by two. This produces a sequence of 6 numbers, that could be rational numbers (in the general sub-Riemannian case, they are), but that are in fact integers. The symbol is this sequence, modulo reflections and cyclic permutations.

The list of possible symbols in the Dido case is a sublist of the list of symbols in the general case. There are 3 possible symbols in place of 7:

THEOREM 3.4. *For generic Dido structures* (*or Riemannian metrics*), *at the isolated degenerate points, the possible symbols for conjugate loci are:*

$$S_1 = (2, 1, 1, 2, 1, 0), \qquad S_2 = (2, 1, 1, 1, 1, 1), \qquad S_3 = (0, 1, 1, 1, 1, 1).$$

These symbols give a complete classification of conjugate loci of degenerate Dido structures, under the action of (*origin preserving*) *homeomorphisms that are smooth together with their inverse, outside the origin.*

This is due to the extra symmetry $\partial/\partial w$. Because of this extra symmetry, high codimension cases, that appeared in the general case disappear. The same holds in the general isoperimetric case.

Another difference with the general case is also (due again to the extra symmetry $\partial/\partial w$): the symbols for conjugate loci are the same for $w > 0$ and $w < 0$. This is true also for the general isoperimetric case, but it is not true in the general sub-Riemannian case, as shown in our paper [4].

As stated in the theorem, the symbol determines completely the conjugate locus, and the rules allowing to recover the conjugate locus from the symbol are the same as for "semi-conjugate loci" of general sub-Riemannian metrics in [4].

Standard arguments of singularity theory show moreover that these symbols are complete invariants under left-right equivalence on $E\backslash\{q_0\}$ of germs of exponential mappings at degenerate points, in restriction to a certain neighbourhood of their (first) singular set.

3.5. CUT LOCI AND SPHERES

Simple general arguments show that, in our case, a point of Cut $L\backslash CL$ is such that several optimal geodesics join this point to the pole at the same arclength-time (see [2]). As a consequence, Cut $L\backslash CL$ is just *the optimal part of the union of self intersections of all wave fronts*.

Therefore, to compute the asymptotics of the cut locus, we just write, for the exponential mapping in suspended form:

$$z_s(\varphi, \sigma, h) - z_s(\varphi', \sigma, h) = 0, \tag{3.18}$$

by definition of the coordinates σ and h. We set $\varphi' = \varphi + \mathrm{d}\varphi$.

In both the degenerate and nondegenerate case, we have asymptotics of the form:

$$z_s(\varphi, \sigma, h) = z_s^n(\varphi, \sigma, h) + o^{n+1}(h, \sigma). \tag{3.19}$$

Obviously, $\sin((\varphi' - \varphi)/2)$ factors out the Equation (3.18), to give an equation of the form:

$$F(\mathrm{d}\varphi, \varphi, \sigma, h) = F^n(\mathrm{d}\varphi, \varphi, \sigma, h) + o^{n+1}(h, \sigma) = 0. \tag{3.20}$$

Setting:
$V_1 = (\cos(\mathrm{d}\varphi/2+\varphi),\ \sin(\mathrm{d}\varphi/2+\varphi))$, $V_2 = (-\sin(\mathrm{d}\varphi/2+\varphi), \cos(\mathrm{d}\varphi/2+\varphi))$, we consider first the equations:

$$F(\mathrm{d}\varphi, \varphi, \sigma, h) \wedge V_1 = 0, \tag{3.21}$$

$$F(\mathrm{d}\varphi, \varphi, \sigma, h) \wedge V_2 = 0. \tag{3.22}$$

The computations show that we can solve the Equation (3.21) with the implicit function theorem (these computations are shown in details in our Appendices 2, 3, for those who know how to read Mathematica). We get an expansion for σ, of the form:

$$\sigma_c = \sigma_c^n(\mathrm{d}\varphi, \varphi, h) + \mathrm{o}(h^{n+1}), \tag{3.23}$$

in which, *as expected*, σ_c^n *has order* 2 *w.r.t.* h. In this expression, $n = 4$ in the nondegenerate case, and $n = 5$ in the degenerate one:

$$\begin{aligned}\sigma_c \ = \ & \frac{\pi}{48}h^2(-72\alpha_0 + 197\alpha_0^2h^2 - 320\tau_2h^2 - \\ & - 120h^2r_2(\cos(2\varphi) + 4\cos(\mathrm{d}\varphi + 2\varphi)) - \\ & - 120h^2r_2\cos(2(\mathrm{d}\varphi + \varphi))) + \mathrm{o}(h^5),\end{aligned} \tag{3.24}$$

$$\begin{aligned}\bar{\sigma}_c \ = \ & \frac{\pi}{48}h^2(-72\alpha_0 + 197\alpha_0^2h^2 - 320\tau_2h^2 - \\ & - 360h^3r_{32}(\sin(3(\mathrm{d}\varphi + \varphi)) + 3\sin(\mathrm{d}\varphi + 3\varphi) + \\ & + 3\sin(2\,\mathrm{d}\varphi + 3\varphi) + \sin(3\varphi)) + \mathrm{o}(h^6).\end{aligned} \tag{3.25}$$

The next step is to replace this estimation in the Equation (3.22). It gives, for the nondegenerate case:

$$h^4(\sin(\mathrm{d}\varphi/2))^2\sin(\mathrm{d}\varphi + 2\varphi) + \mathrm{o}(h^5) = 0, \tag{3.26}$$

and for the degenerate case:

$$h^5(\sin(\mathrm{d}\varphi/2))^2\cos(\mathrm{d}\varphi/2)\cos(3/2(\mathrm{d}\varphi + 2\varphi)) + \mathrm{o}(h^6) = 0. \tag{3.27}$$

Remark (about formulas (3.26), (3.27)). The term $\sin(\mathrm{d}\varphi/2)$ is easy to understand: it corresponds to the conjugate locus, which obviously should also satisfy our equations for $\mathrm{d}\varphi = 0$. It correspond also to singularities of the wave fronts that are cuspidal lines.

LEMMA 3.5. *In formulas* (3.26), (3.27), *the term* $(\sin(\mathrm{d}\varphi/2))^2$ *factors out.*

Proof. We use the notations in force from the beginning of this section. We have to solve an equation of the type:

$$\frac{z_s(\varphi', \sigma) - z_s(\varphi, \sigma)}{\sin((\varphi' - \varphi)/2)} = F(\varphi', \varphi, \sigma) = 0,$$

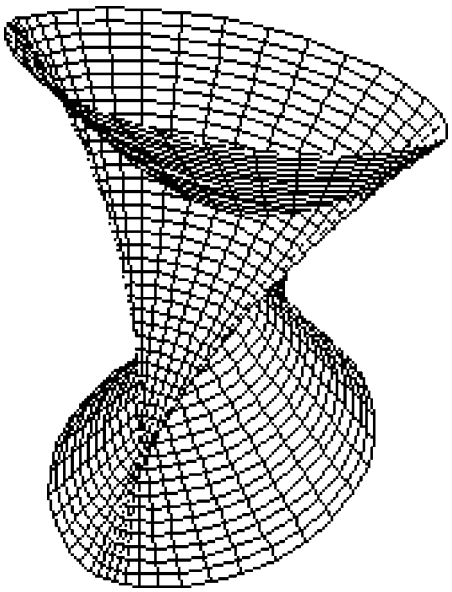

Figure 6. Wave front, nondegenerate case.

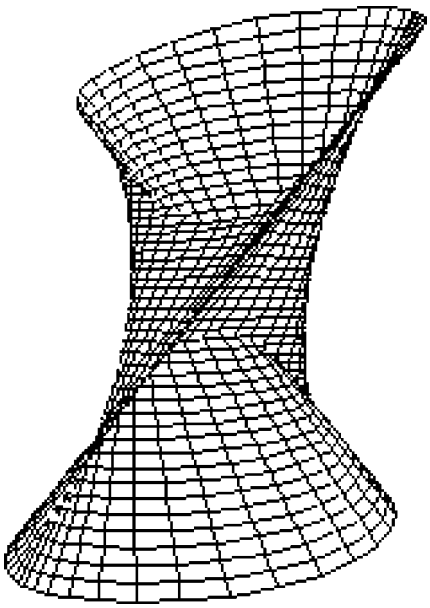

Figure 7. Wave front, nondegenerate case.

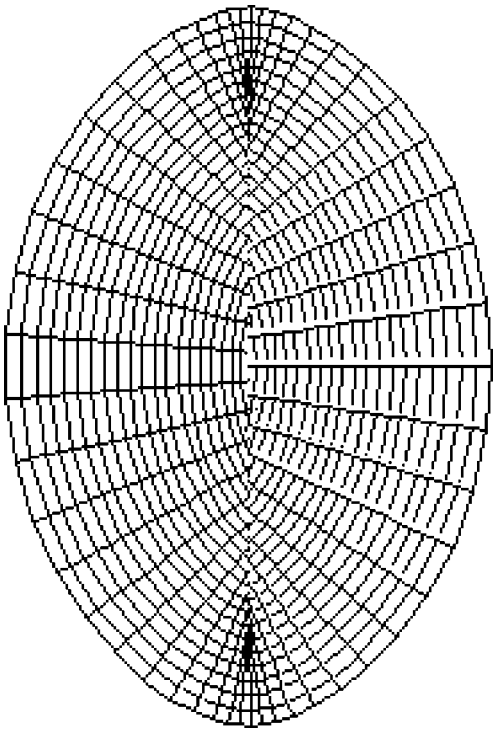

Figure 8. Wave front from above, nondegenerate case.

where $F(\varphi', \varphi, \sigma)$ is smooth, $F(\varphi', \varphi, \sigma) = F(\varphi, \varphi', \sigma)$ and $F(\varphi, \varphi, \sigma) = 2\frac{\partial z_s}{\partial \varphi}(\varphi, \sigma)$. Moreover, if ω is the Liouville form restricted to $H_{1/2}$,

$$\omega(\exp s\mathbf{H}(\varphi, \rho)) = \frac{1}{\rho(\varphi, \sigma, h)}(\tilde{\omega}\,\mathrm{d}z + 2\pi h\,\mathrm{d}h).$$

For $\tilde{\omega}$, we have the trivial smooth estimate: $\tilde{\omega} = h\cos(\varphi)\,\mathrm{d}x + h\sin(\varphi)\,\mathrm{d}y + \mathrm{o}(h^2)$. Let us chose again the two vectors of R^2:

$$V_1(\varphi', \varphi) = \left(\cos\left(\frac{\varphi' + \varphi}{2}\right), \sin\left(\frac{\varphi' + \varphi}{2}\right)\right),$$
$$V_2(\varphi', \varphi) = \left(-\sin\left(\frac{\varphi' + \varphi}{2}\right), \cos\left(\frac{\varphi' + \varphi}{2}\right)\right).$$

Note that $V_1(\varphi', \varphi) = V_1(\varphi, \varphi')$, $V_2(\varphi', \varphi) = V_2(\varphi, \varphi')$, and if V is any nonzero vector, the relations $V_1(\varphi, \varphi) \wedge V = 0$ and $\tilde{\omega}(V) = 0$ cannot hold simultaneously for h sufficiently small. We know that the equation $V_1(\varphi', \varphi) \wedge F(\varphi', \varphi, \sigma) = 0$ has a smooth solution $\sigma_c(\varphi', \varphi)$: this is just the Equation (3.21). Also, by symmetry, $\sigma_c(\varphi', \varphi) = \sigma_c(\varphi, \varphi')$. Now, set $V = \frac{1}{2}F(\varphi, \varphi, \sigma_c(\varphi, \varphi)) = \frac{\partial z_s}{\partial \varphi}(\varphi, \sigma_c(\varphi, \varphi))$. We also know that $\tilde{\omega}_{|\varphi, \sigma_c(\varphi, \varphi)}(V) = 0$ (see the proof of Lemma 3.1). Therefore, simultaneously $\tilde{\omega}(V) = 0$ and $V_1(\varphi, \varphi) \wedge V = 0$. Hence, $V = 0$. It follows from the Lemma 3.1 that, in fact, $\sigma_c(\varphi, \varphi) = \sigma_{\mathrm{conj}}(\varphi)$, the conjugate time.

Set $F(\varphi', \varphi, \sigma_c(\varphi', \varphi)) = \tilde{F}(\frac{\varphi'-\varphi}{2}, \frac{\varphi'+\varphi}{2}) = \tilde{F}(u, v)$. By the definition of F, $\tilde{F}(-u, v) = \tilde{F}(u, v)$.

Therefore, $\tilde{F}(u, v) = \tilde{F}_0(v) + u^2\tilde{F}_1(u, v)$. But, $\tilde{F}_0(v) = \tilde{F}(0, \varphi) = F(\varphi, \varphi, \sigma_c(\varphi, \varphi)) = \frac{\partial z_s}{\partial \varphi}(\varphi, \sigma_c(\varphi, \varphi)) = 0$. This shows that $F(\varphi', \varphi, \sigma_c(\varphi', \varphi)) = (\varphi' - \varphi)^2\bar{F}(\varphi', \varphi)$, for a certain smooth function $\bar{F}(\varphi', \varphi)$. Therefore, $(\varphi' - \varphi)^2$ factors out in the Equation (3.22) in which one plugs the solution (3.23) of the Equation (3.21). □

Hence our Equations (3.26), (3.27) can be rewritten:

$$\sin(\mathrm{d}\varphi + 2\varphi) + \mathrm{o}(h) = 0, \tag{3.28}$$

$$\cos(\mathrm{d}\varphi/2)\cos(3/2(\mathrm{d}\varphi + 2\varphi)) + \mathrm{o}(h) = 0. \tag{3.29}$$

Let us first do the job in details in the non degenerate case, and second, just explain the difficulties and state the results in the degenerate one.

By the implicit function theorem, the Equation (3.28) has two smooth solutions, for h small enough:

$$\mathrm{d}\varphi_1 = -2\varphi + \mathrm{o}(h), \qquad \mathrm{d}\varphi_2 = -2\varphi + \pi + \mathrm{o}(h). \tag{3.30}$$

Replacing these expressions in (3.24), we get two smooth functions of h, φ, that are estimates of the cut time, the difference between them is $20h^4\pi r_2$, which shows that one only can be optimal. It corresponds to $\mathrm{d}\varphi_1$, and is given by:

$$\begin{aligned}\sigma_{\mathrm{cut}} \;=\; & h^2\pi(-72\alpha_0 + 197\alpha_0^2h^2 - 160h^2(3r_2 + 2\tau_2) - \\ & - 240h^2r_2\cos(2\varphi))/48 + \mathrm{o}(h^5).\end{aligned} \tag{3.31}$$

The corresponding estimate of the cut-locus is:

$$z_{\mathrm{cut}} = h^4\pi(3r_1\sin(t1) - 20hr_2\cos(\varphi), 3r_1\cos(t1)) + \mathrm{o}(h^6). \tag{3.32}$$

Similarly to the conjugate locus, it is shifted by a vector which is normal to the gradient of the curvature, of order h^4, and it has size h^5.

This estimate is drawn, together with (a section at $h = cst$ of) the conjugate locus on the Figure 5.

Also, at this step, it is interesting to watch the shape of the estimates of the wave fronts (and spheres) of small radius, in a neighbourhood of the Heisenberg conjugate time, $t_H = 2\pi$. These estimates can be drawn just by plugging $\sigma = \frac{s-2\pi h}{h}$ in the formulas (3.7), (3.8). This has been done, to get the Figures 6, 7, 8.

As we see on the Figures 5, 8 (and as is expected), the boundary of the cut-locus coincides with cusps of the conjugate locus. This can be seen from the general theory of Legendre singularities: it can be checked that we get on the wave fronts four swallow tails, connected by four cuspidal lines, that are stable Legendre singularities. This also can be seen directly. Let us show only the following:

LEMMA 3.6. *The boundary of the cut locus coincides with the cuspidal lines of the conjugate locus* (*i.e., at these points, there are swallow tails on wave fronts*).

Proof. First the difference $d(\varphi)$ between the conjugate time and cut time estimates (relative to $\mathrm{d}\varphi_1$) is > 0 as expected, out of a neighbourhood of cusps: $\mathrm{d}(\varphi) = 20\pi h^4 r_2 \sin(\varphi)^2 + \mathrm{o}(h^5)$.

We have three functions under consideration: (1) the conjugate time function, $\sigma_{\mathrm{conj}}(\varphi, h)$, (2) the self-intersection function, called above σ_{cut}, but called $\sigma_i(\varphi, h)$ here, (3) the cut time function $\sigma_{\mathrm{cut}}(\varphi, h)$, i.e., the first time at which the geodesic (φ, h) ceases to be globally optimal. Here, $\sigma_{\mathrm{conj}}(\varphi, h)$, $\sigma_i(\varphi, h)$ are smooth functions, and for h fixed, sufficiently small, both of them attain strict local minima $\sigma_{\mathrm{conj}}(\varphi_c(h), h)$, $\sigma_i(\varphi_i(h), h)$ in a neighbourhood of $\varphi = 0$ (we treat the case $\varphi = 0$ only, the case $\varphi = \pi$ is similar). It follows from the general theory (see for instance [2]) that: (a) after $\sigma_{\mathrm{conj}}(\varphi, h)$, the geodesic (φ, h) is no more locally optimal, (b) $\sigma_{\mathrm{cut}}(\varphi, h)$ is either equal to $\sigma_{\mathrm{conj}}(\varphi, h)$, or to $\sigma_i(\varphi, h)$. Therefore, $\sigma_{\mathrm{cut}}(\varphi, h) = \inf(\sigma_{\mathrm{conj}}(\varphi, h), \sigma_i(\varphi, h))$.

Assume that for some φ, $\sigma_i(\varphi, h) > \sigma_{\mathrm{conj}}(\varphi, h)$, then, $\sigma_i(\varphi, h)$ is not the optimal time, and the same is true for the (unique) φ' such that $\sigma_i(\varphi, h) = \sigma_i(\varphi', h)$. Therefore, $\sigma_i(\varphi', h) > \sigma_{\mathrm{conj}}(\varphi', h)$. Let us call this fact (F_1). The second fact (F_2) is that $\sigma_{\mathrm{conj}}(\varphi_i(h), h) = \sigma_i(\varphi_i(h), h)$. We will prove it in a moment. This, with fact (F_1) implies that $\varphi_i(h) = \varphi_c(h)$. Therefore, either $\sigma_{\mathrm{cut}}(., h) = \sigma_{\mathrm{conj}}(., h)$, or $\sigma_{\mathrm{cut}}(., h) = \sigma_i(., h)$. The formulas show that the difference $\sigma_i(\varphi, h) - \sigma_{\mathrm{conj}}(\varphi, h) = -20h^4\pi r_2 \sin(\varphi)^2 + \mathrm{o}(h^5)$ is also a smooth function, with a local strict maximum, for φ close to zero. This maximum is zero, hence, $\sigma_{\mathrm{cut}}(\varphi, h) = \sigma_i(\varphi, h)$. For h fixed, $\sigma_{\mathrm{conj}}(\varphi, h)$ and $\sigma_{\mathrm{cut}}(\varphi, h)$ are smooth functions, with the same strict local minimum at $\varphi_i(h) = \varphi_c(h)$.

We already know by our Lemma 3.1 that $\varphi_c(h)$ corresponds to a cusp of the conjugate locus, and it is obvious now that $\varphi_i(h)$ corresponds to a point of the boundary of the cut locus.

It remains only to show that (F_2) holds.

This is more or less obvious: fixing h, there are sequences φ_n, φ_n', both converging to $\varphi_0 = \varphi_i(h)$, and a sequence σ_n, converging to $\sigma_0 = \sigma_i(\varphi_i(h), h)$, such that $\frac{z(\varphi_n', \sigma_n) - z(\varphi_n, \sigma_n)}{\varphi_n' - \varphi_n} = 0$. The limit has to be $\frac{\partial z}{\partial \varphi}(\varphi_0, \sigma_0)$. Hence $\frac{\partial z}{\partial \varphi}(\varphi_0, \sigma_0) = 0$. By the Lemma 3.1, $z(\varphi_0, \sigma_0)$ has to be a conjugate point. □

Note 13. In the previous lemma, we gave the proof for the cut locus, but a (trivial) variation of this proof also works for the non-optimal part of the self-intersection of the wave fronts (corresponding to $\mathrm{d}\varphi_2$ in (3.30)), because it corresponds also to local extrema of the cut time and conjugate time. The boundary of this nonoptimal part coincides with the remaining two cusp points of the conjugate locus.

THEOREM 3.7 (Cut locus and sphere in the nondegenerate case). *The cut time and the cut locus have the smooth asymptotics* (3.31), (3.32). *In particular, the cut locus has size* h^5 (*in place of* h^3 *for generic sub-Riemannian metrics or generic isoperimetric problems*).

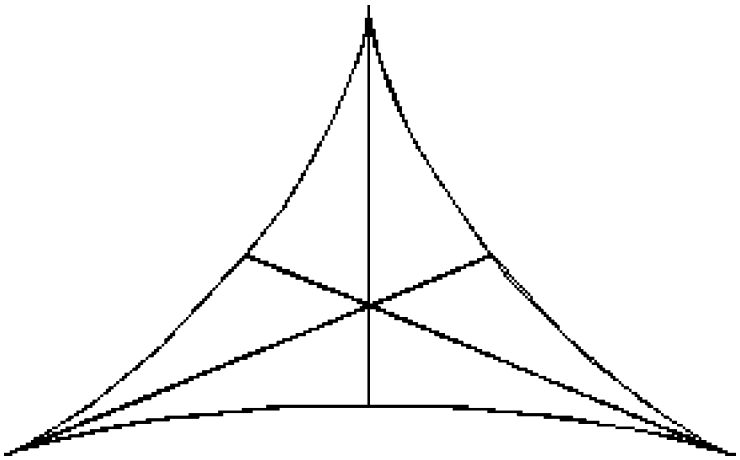

Figure 9. Degenerate case, 1st part of the self-intersection of the wave front.

Sections by $h = cst$ of the cut-locus are curve segments joining two cusp points among those of the conjugate locus.

The small spheres are homeomorphic to Euclidean spheres, but they are not smooth: the subset where they are not differentiable consists of two curve segments.

Singularities of the small wave fronts, that are close to the sphere are shown on the Figures 6, 7, 8. *The Figure* 8 *also shows the shape of the spheres seen from above* (*in normal isoperimetric coordinates*).

Asymptotics for the singular part of the spheres and the first singularities of the wave fronts are given by the asymptotics of the exponential mapping (3.7), (3.8) *in which one plugs $\sigma = \frac{s-2\pi h}{h}$, s the radius. For the sphere, moreover, $\sigma_{\text{cut}}(\varphi, h) \geqslant \frac{s-2\pi h}{h}$.* (*In these asymptotics, we consider $w > 0$ only, the upper hemisphere.*)

The singularities of the typical small wave front fall in two parts (*upper and lower hemisphere*). *Each of them consists of a closed cuspidal curve, with 4 cusp points. At the cusp points appear swallow tails. On each part, there are also two curve segments* (*each of them joining two of the cusp points*), *the nonboundary points of these segments correspond to transversal self-intersections of the wave front. One of these segments is the* (*upper or lower*) *singular set of the sphere.*

Now, let us study more briefly the *degenerate case*. All computations are done in details in the program of our Appendix 3, and are easy to follow.

The results are more complicated, and more difficult to understand, due to the already mentioned asymptotic symmetry, mainly.

Difficulties start with the formula (3.29): for the values $\varphi = k\pi/3$ and $\mathrm{d}\varphi = \pi$, the two terms vanish simultaneously. This is, as we shall see, the first effect of the asymptotic symmetry, and will be the cause of unstable phenomena at this level of approximation, which disappear when considering higher order jets. The point is that these phenomena are of no importance for the spheres, and the optimal synthesis. They play a role for singularities of wave fronts only.

If we are interested only with the optimal synthesis (the cut-locus and the spheres), then, we can easily forget this difficulty, as follows:

– first, in a neighbourhood of the points $\varphi = k\pi/3$, we have a number of well defined self-intersection-time functions $\sigma_{s,i}(\varphi, h)$: those obtained by solving the Equation (3.29), when $\mathrm{d}\varphi$ *is not close to* π, i.e. $\mathrm{d}\varphi_i(\varphi, h) = -2\varphi + (2i+1)\pi/3 + \mathrm{o}(h)$, $i \neq k + 3l + 1$ for some integer l.

– second, using the smooth expression $\bar{\sigma}_c = \sigma_c^5(\mathrm{d}\varphi, \varphi, h) + \mathrm{o}(h^6)$, (3.23), for the values $\mathrm{d}\varphi = \pi + \varepsilon$, ε small, we can compare this expression to the values corresponding to $\mathrm{d}\varphi_i(\varphi, h)$:

Set $\Delta_i(\varphi, h, \varepsilon) = \sigma_{s,i}(\varphi, h) - \bar{\sigma}_c(\pi + \varepsilon, \varphi, h)$. Computations give:

$$\Delta_i(\varphi, h, \varepsilon) = -60h^5\pi r_{32}(-1)^i \cos\left(\varphi - \frac{\pi}{6}(2i+1)\right) + \mathrm{o}(h^6) + \mathrm{o}(h^5\varepsilon),$$

$$\Delta_i\left(k\frac{\pi}{3}, h, \varepsilon\right) = -60h^5\pi r_{32}(-1)^i \cos\left(\frac{\pi}{6}(2(k-i)-1)\right) + \mathrm{o}(h^6) + \mathrm{o}(h^5\varepsilon). \tag{3.33}$$

This shows that, in adequate neighbourhoods of these points $\varphi = k\pi/3$ and $\mathrm{d}\varphi = \pi$, this difference can be made strictly smaller than $-ah^5$, for $a > 0$, constant. Hence, $\sigma_{s,i}(\varphi, h)$ will always be smaller than the solution for $\mathrm{d}\varphi$ close to π, if any. We conclude that the cut-time is among the well defined solutions $\sigma_{s,i}(\varphi, h)$, or is the conjugate time.

When φ is not close to $k\pi/3$, the solution corresponding to $\mathrm{d}\varphi$ close to π is well defined, smooth, and is:

$$\begin{aligned} &\mathrm{d}\varphi_\pi = \pi + \mathrm{o}(h); \\ &\sigma_\pi(\varphi, h) = h^2\pi(-72\alpha_0 + 197\alpha_0^2 - 320h^2\tau_2)/48 + \mathrm{o}(h^6). \end{aligned} \tag{3.34}$$

Again, it is easy to compare this solution to the $\sigma_{s,i}(\varphi, h)$, and to check directly that it is in fact never optimal. By comparison with the conjugate time, it is also easy to show (except near cusp points of the conjugate locus), that the cut time is among the $\sigma_{s,i}(\varphi, h)$.

What happens in a neighbourhood of cusp points of the conjugate locus, is exactly similar to the nondegenerate case (the proofs work without any modification). Again, these points correspond to swallow tails on the wave fronts.

At the end, we get the following estimates, for the cut-time and cut locus:

$$\begin{aligned} \mathrm{d}\varphi_i(\varphi, h) &= -2\varphi + (2i+1)\pi/3 + \mathrm{o}(h), \\ \sigma_{s,i}(\varphi, h) &= \bar{\sigma}_c^5(\mathrm{d}\varphi_i(\varphi, h), \varphi, h) + \mathrm{o}(h^6), \\ \sigma_{\mathrm{cut}}(\varphi, h) &= \mathrm{Inf}_i(\sigma_{s,i}(\varphi, h)), \\ z_{\mathrm{cut}}(\varphi, h) &= \bar{z}_s(\varphi, \sigma_{\mathrm{cut}}(\varphi, h), h), \end{aligned} \tag{3.35}$$

where $\bar{\sigma}_c^5$ comes from (3.25), where $\bar{z}_s$ is given in formulas (3.9), (3.10), $i = 1, 2$ or 3.

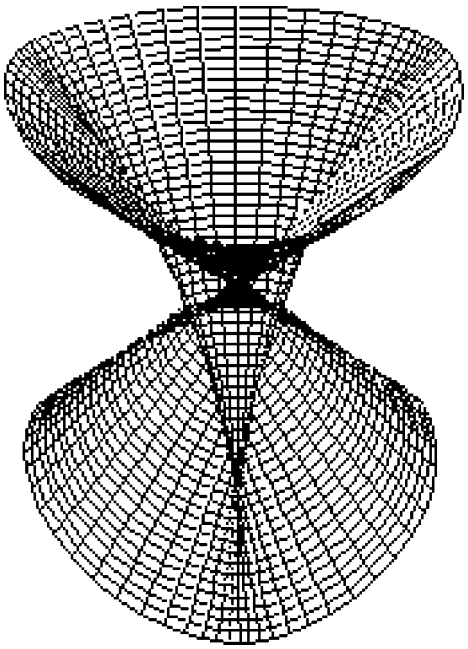

Figure 10. Degenerate case, wave front.

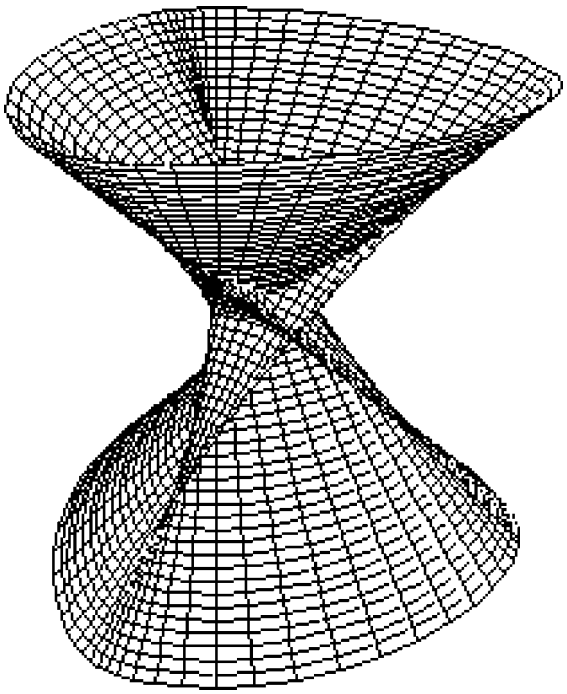

Figure 11. Degenerate case, wave front.

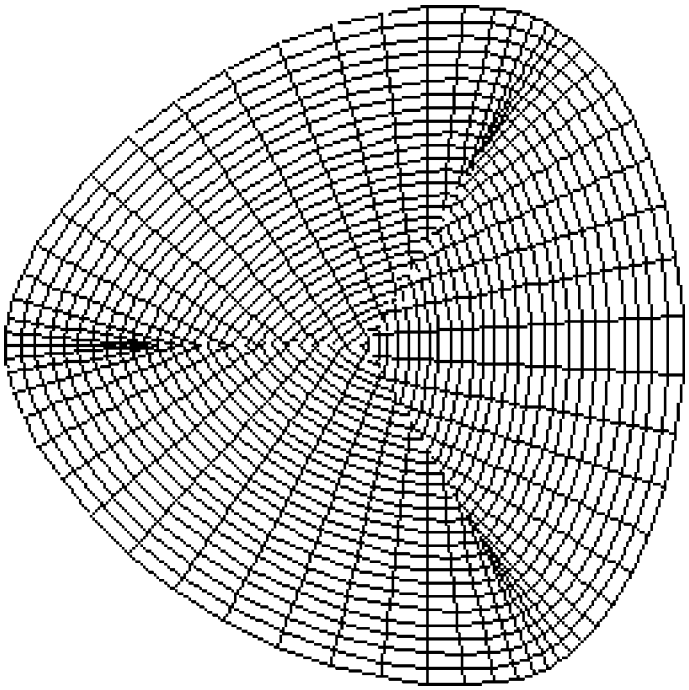

Figure 12. Degenerate case, wave front from above.

The Figure 9 shows the interesting part (called *Part* 1) of the self-intersection of the wave fronts (i.e., the union of the 3 images of the mappings $\bar{z}_s(\varphi, \sigma_{s,i}(\varphi, h), h)$). The Figures 10, 11, 12 show the interesting part of the wave fronts (i.e., the part close to $t_H = 2\pi$, the Heisenberg conjugate time).

It is easy to check that the 3 (estimate) pieces of the self intersection Part 1 of the wave fronts are 3 *quadruple* curves, which intersect at a single point (the equations are given in the Appendix 3, or can be computed easily by the hand). The curves are double because any self-intersection curve should be double, and they are quadruple because of the asymptotic symmetry. The intersection of this locus with a single wave front, is a curve which is double only.

On the Figure 9, we see these 3 pieces, together with the conjugate locus. Examining the wave front, on the Figures 10, 11, 12, we see that the common intersection of these 3 curves is a stable phenomenon: it corresponds to transversal intersection of 3 surfaces. It is clear that the sections of the cut locus by $h = cst$ are formed by 3 segments, issued from a single point, and the other endpoints of these segments correspond to 3 among the base points of the 6 swallow tails appearing on the wave fronts.

THEOREM 3.8 (Cut locus and sphere at degenerate points). (1) *The cut angle, cut time and cut locus have the asymptotics* (3.35). *In particular, the cut locus has*

size h^6 (*in place of* h^4 *in the case of generic sub-Riemannian metrics, or generic isoperimetric problems*).

(2) *Sections of the cut locus by* $h = cst$ (*and not only their asymptotics*) *consist of* 3 *curve segments with a common endpoint.*

(3) *The other endpoints of the* 3 *segments coincide with cusps of the conjugate locus.* (*Again, this is true for the cut locus and not only for the asymptotics, despite the fact that the conjugate locus is not well described at this level of approximation.*)

(4) *The small spheres are homeomorphic to Euclidean spheres, but they are not differentiable. The singular set of the sphere falls in two pieces* (*in both hemispheres*), *each of them consisting of 3 curve segments, with one common endpoint. The other endpoints are basepoints of swallow-tails on the corresponding wave fronts.*

As we announced, the remarkable fact is that *the degeneracy due to this asymptotic symmetry does not play any role for spheres and cut loci.*

On the contrary, it does play an important role for the wave front and its self-intersection. The first point is about the second part *Part* 2 of the self-intersection, i.e., the part corresponding to the asymptotics (3.34). This part is shown on the Figure 13, together with the conjugate locus. It is also a double curve presenting 3 cusp points.

The most unstable thing of this approximation of the wave-front is at the level of these cusp points on Part 2. They correspond to $\varphi = k\pi/3$, i.e. to the bad points treated above, for which we just concluded to nonoptimality.

After breaking the symmetry with higher order jets, the conjugate locus will become a simple curve, with 6 cusp points and transversal self-intersections.

One can see on the Figure 11 that the cuspidal closed singular curve on the wave front (with 6 cusps points) has 3 self-intersections (one of them is shown on the figure). This is unstable. These points coincide with the cusp points of Part 2.

In fact, after breaking the symmetry, we will just get 3 times 2 cusps (closer and closer when h goes to zero). Even with the computer, it is difficult to show what happens, but it is easy to understand.

THEOREM 3.9 (Wave front at degenerate points). *The singularities of the wave fronts that are close to the corresponding spheres fall in two pieces* (*upper and lower hemisphere*). *One of these pieces is shown on the Figures* 10, 11, 12. *It consists of:*

(1) *a closed cuspidal curve with* 6 *cusp points, that are basepoints of* 6 *swallow tails. At the level of the approximation* $\bar{z}_s^6(\varphi, \sigma, h)$, *there are* 3 *self-intersection points on this closed curve, which disappear at higher order approximation for a generic problem.*

(2) *There is a certain self-intersection locus, with endpoints on the* 6 *swallow tails, and with* 6 *cusps. The intersection of this locus and the cut locus is the singular set of the sphere.*

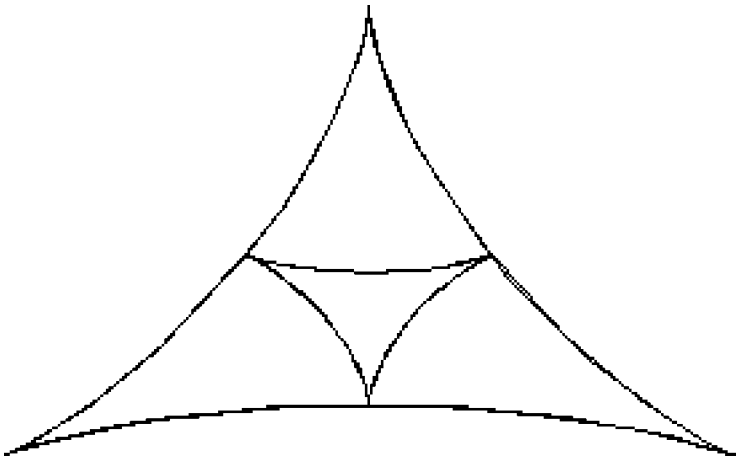

Figure 13. Degenerate case: Part 2 of the self-intersection of the wave front.

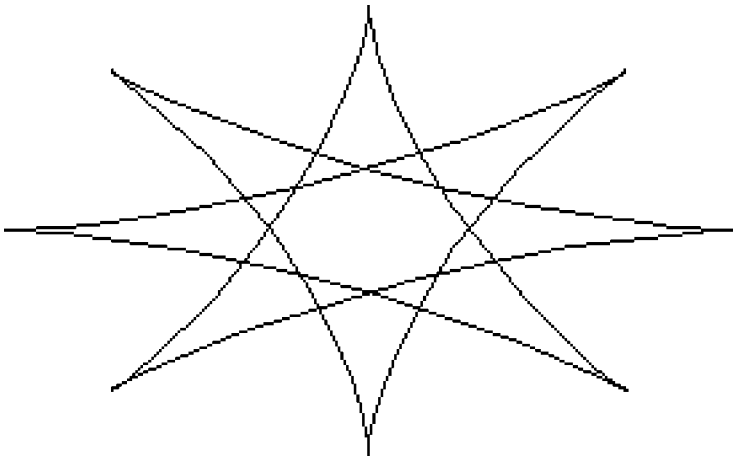

Figure 14. Conjugate locus, 8 cusps.

4. Complements

4.1. GETTING AN ARBITRARILY LARGE NUMBER OF CUSPS

In the generic situation, the number of cusps of the conjugate locus, n_{cusp} is equal to the double of the number of free endpoints of the singular segments on the hemisphere, n_e, and is also equal to the number n_{sw} of swallow tails close to the (hemi)sphere on the (hemi)wave front of same radius

$$n_{\text{cusp}} = 2n_e = n_{sw}. \tag{4.1}$$

Also $n_{\text{cusp}}/2$ is equal to the first integer $j > 1$ such that $\nabla_j^j k(q_0) \neq 0$, where k is the Gaussian curvature, q_0 is the pole, and the notation for the decomposition

of tensors is the one given in Section 2.8. It seems that there is something general beyond these facts.

OPEN PROBLEM. (For any (nongeneric) germ at q_0 of Riemannian metric which is "nonflat" in the sense that, for some integer $i > 1$, $\nabla_i^i k(q_0) \neq 0$.) Set $j =$ first integer > 1 such that $\nabla_j^j k(q_0) \neq 0$. Is it still true that:

(a) $n_{\text{cusps}} = 2\ j$?
(b) the formula (4.1) holds?
(c) if j is odd, then the conjugate locus is asymptotically double?

The same problem also makes sense in the general case of (isoperimetric or not) sub-Riemannian metrics.

Perhaps, accordingly to the generic cases, this term $\nabla_j^j k(q_0)$ *dominates* all other terms. We are unable to prove this in general. Nevertheless, what we can do is to compute the conjugate locus for a (germ of) Riemannian metric such that all tensors are 0, in the decomposition of the successive covariant derivatives of the curvature, except one: $\nabla_j^j k(q_0)$ for some j.

We did this computation, for $j = 4$, and for $j = 5$.

We obtained the following asymptotics, in normal coordinates, for the conjugate locus:

$$j = 4: \tag{4.2}$$
$$x_{\text{conj}}(\varphi, \rho) = \rho^5 \cos(\varphi)^3(-2 + 3\cos(2\varphi)),$$
$$y_{\text{conj}}(\varphi, \rho) = -\rho^5 \sin(\varphi)^3(2 + 3\cos(2\varphi)).$$

$$j = 5: \tag{4.3}$$
$$x_{\text{conj}}(\varphi, \rho) = 8\rho^6 \cos(\varphi)^3(-3\sin(\varphi) + 2\sin(3\varphi)),$$
$$y_{\text{conj}}(\varphi, \rho) = \rho^6(3\cos(4\varphi) - 2\cos(6\varphi)).$$

Both asymptotics of these conjugate loci are drawn on the Figures 14, 15.

4.2. COLLISION OF PARTICLES IN A STRONG MAGNETIC FIELD

It is explained in [15], that the motion of a particle in a magnetic field over a 2-d Riemannian manifold M is related with the above considerations. If we have a principal circle bundle E over M, with a connection, α being the connection form, $\mathrm{d}\alpha$ defines a 2-form η on M. The value ψ of the magnetic field is defined by $\eta = (\text{Volume})\psi$. The motion $z(s)$ of a particle with charge c is described by:

$$k_g(z(s)) = c\psi(z(s)), \tag{4.4}$$

where $k_g(z(s))$ is the geodesic curvature of $z(s)$.

It is easily checked that this equation is exactly the equation of projections on M of the geodesics of our corresponding isoperimetric metric: using the isoperimetric

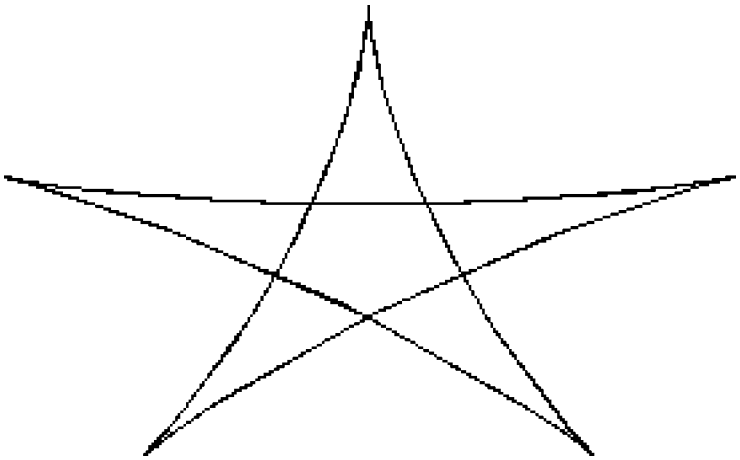

Figure 15. Conjugate locus, 10 cusps (asymptotic symmetry).

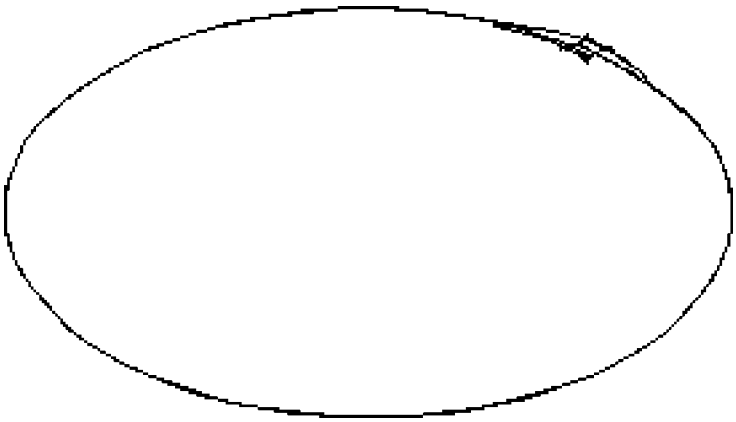

Figure 16. Nondegenerate case, collision locus.

normal form (2.11), it is sufficient to check that (4.4) is verified at the pole. But at the pole, $\frac{\nabla(\dot{z}(s))}{\mathrm{d}s} = \frac{\mathrm{d}^2 z(s)}{\mathrm{d}s^2}$ because coordinates on the quotient are just standard normal Riemannian coordinates. Five lines of small computations with the normal form give the result.

Here, we study only the case of constant charge particles in a strong magnetic field. The field has to be much stronger than the charge in order to neglect interactions, because we are interested with the simultaneous motion of several particles and their collision. We work with a constant magnetic field, which corresponds to the Dido case. The same work can be done for generic isoperimetric problems, i.e. non constant magnetic field. It leads to similar results (at different scales).

If several particles with same charge and same speed are emitted from the pole at time zero in different directions, then, collisions can happen in arbitrary short time. The locus where such collisions appear we call the "collision locus". Computing

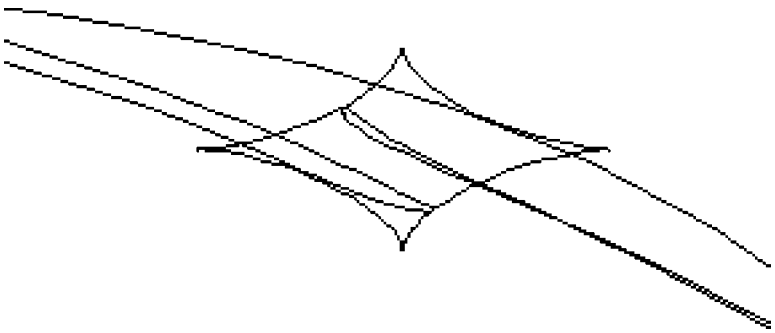

Figure 17. Nondegenerate case, collision locus (near conjugate locus).

the collision locus is clearly a problem very similar to the one of computing the cut locus of the underlaying sub-Riemannian metric. We only want to point out the apparently *strange following fact*: The collision locus is very different from the cut locus: it has size h^4 in place of h^5 in the nondegenerate case, and h^5 in place of h^6 in the degenerate case. Hence, it is even much bigger than the conjugate locus.

We will not say much here in. We will just state results and show pictures.

If the charge is 1, $r = 1/\rho$ is the magnetic field. The trajectories are projections on M of geodesics of our isoperimetric metric. The map under consideration is now the map $z(s, \varphi, \rho)$. Set $z_\rho(s, \varphi) = z(s, \varphi, \rho)$. The collision locus is the set of points at the image of the map z_ρ, that are double with respect to φ, exactly as the cut locus is the set of points at the image of the map $z_h(s, \varphi) = z(s, \varphi, h)$, that are double with respect to φ.

The two following points are important:

(a) we can consider our Hamiltonian H as a Hamiltonian on T^*M, depending on ρ. (Note that this Hamiltonian H_ρ is no more homogeneous.) The trajectories of the motion are trajectories of $\mathbf{H}_\rho$.

(b) It can be easily computed that the singular set of this map z_ρ has *the same asymptotic expansion as the conjugate locus* of the sub-Riemannian metric (note that it is not clear that it is exactly the same). The cusps that appear in this expansion are stable for the same reasons as previously: They are just singularities of the ordinary map z_ρ: $R^2 \to R^2$, and this map is Whitney.

We can compute asymptotics for the collision locus using exactly the same method as for the cut-locus. We did this for both the degenerate and nondegenerate case. Results are more complicated, hence we don't show formulas.

As we said, although the singular locus is the same as the conjugate locus (*with same size*), the collision locus has order *one less* (with respect to ρ or equivalently w.r.t. h).

On the Figures 16, 17, we show the non-degenerate case (the Figure 17 is a zoom at the level of the conjugate locus, which is also the set of singular values of the map z_ρ). The Figure 18 shows the degenerate case.

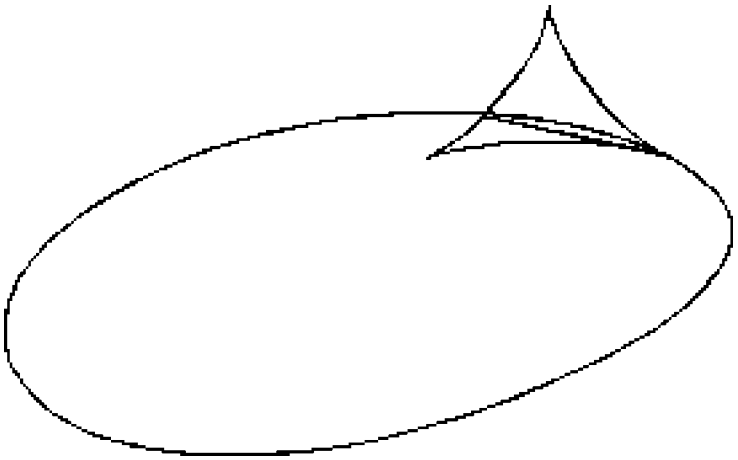

Figure 18. Degenerate case, collision locus.

Appendices. All the programs were developed under Mathematica 3.0

Appendix 1

Here is the program computing the asymptotic expansion with respect to ρ of the exponential mapping, given by the formulas (2.22), (2.23). The results are at the end of the program. The computation is done at the higher order we need, but last terms assume that $\nabla_2^2 k = 0$. The method is the brute force method explained in the Section 3.1. We do not print all results here, because some of them are too long. For instance, the expressions of ε_5^z, ε_6^z, are several pages long. The reader has to execute the program to get them.

```
Expnd1[F_,n_,x_,y_,z_,w_,u_,pds_] := (GGG = F /. {x->ttt^ pds[[1]] x,y->ttt^ pds[[2]]
y, z-> ttt^ pds[[3]] z, w->ttt^ pds[[4]] w,u->ttt^ pds[[5]] u};GGG1 = Table[0, {i,1,n+1}];
GGG2 = GGG /.ttt->0;GGG1[[1]] = GGG ;Do[(GGG1[[i]] =D[GGG1[[i-1]]/(i-1),ttt];
GGG2 = GGG2 + (GGG1[[i]]/.ttt->0)),{i,2,n+1}];GGG2 ) ;Expnd[F_,n_,x_,y_,z_,w_,u_,
pds_] := (GGG =F /. {x->ttt^ pds[[1]] x,y->ttt^ pds[[2]] y,z- ttt^ pds[[3]] z, w->ttt^ pds[[4]]
w,u->ttt^ pds[[5]] u};GGG1 = Table[0, {i,1,n+1}];GGG1[[1]] =GGG ;Do[GGG1[[i]] =
D[GGG1[[i-1]]/ (i-1), ttt], {i, 2,n+1}]; GGG1 /.ttt->0 );

Eat[t_] := {{Cos[t/2]^ 2, Sin[t]/2, Sin[t], 2 Sin[t/2]^ 2} ,{-Sin[t]/2, Cos[t/2]^ 2, -2 Sin[t/2]
^ 2 ,Sin [t] }, {- Sin[ t]/4, - 1/2 Sin[t/2]^ 2, Cos[t/2]^ 2, Sin[t]/2},{1/2 Sin[t/2]^ 2, -Sin[t]/4,
-Sin[t]/2, Cos [t/2 ]^ 2 }}; Z1 [t_] := {2 * Cos[phi - t/2]*Sin[t/2],2*Sin[phi - t/2]*Sin[t/2],
Cos[phi - t/2]*Cos[t/2],Cos[t/2]*Sin[phi - t/2]};

Alpha= Alpha0 + Alpha1 + Alpha2+Alpha3;Alpha1 = r1(Cos[t1] x -Sin[t1] y);Alpha2
= to2 (x^ 2 + y^ 2 ) + r2(Cos[t2](x^ 2-y^ 2)-2 Sin[t2] x y);Alpha3 = r31 (x^ 2 + y^ 2)(Cos[t31]
x + Sin[t31] y) +r32(Cos[t32] x(x^ 2-3 y^ 2) - Sin[t32] y* (3 x^ 2-y^ 2)); t32 = 0; Gaux
=1 /(1+ ttt^ 2 (x^ 2+ y^ 2)*(Alpha/. {x-> ttt x, y-> ttt y}));Gaux1 = Expnd1[Gaux,5,
ttt, aaa1,aa2,aaa3,aaa4,{1,1,1,1,1}]; Gaux2 = Integrate[2 ttt Gaux1, {ttt,0,1}];Gaux3 =
```

```
(1+(x^2+y^2) Alpha) Gaux2;Gaux4 = Expnd1[Gaux3, 5, x,y,aa1,aa2,aa3,{1,1,1,1,1}];w1 = y/2 Gaux4; w2 = -x/2 Gaux4;x1 = 1 + y^2 Alpha; y1 = -x y Alpha;x2 = - x y Alpha;y2 = 1 + x^2 Alpha;
    Le Hamiltonien, H. Le champ Hamiltonien dont les
    composantes sont Hx, Hy, Hw, Hp, Hq, Hr, par rapport
    au nouveau temps, dt = r(s) ds, s = longueur d'arc.
    ******************************************
    H = 1/2 (p x1 + q y1 +r w1)^2 + 1/2 (p x2 + q y2 + r w2)^2; Hx = D[H,p]; Hy = D[H, q]; Hp = - D[H, x]; Hq = -D[H,y];Hx = Hx /. r ->1; Hy = Hy /. r ->1;Hp = Hp /. r ->1; Hq = Hq /. r->1;Hw = D[H,r]; Hw = Hw/. r->1;Hflechew = Expnd[Hw,7, x,y,p,q,aaa1, {1,1,1,1,1}];Hflechew = Simplify[Hflechew/. t2->0];Hflechew= InputForm[Hflechew]
    Hflechex =Expnd1[Hx,6,x,y,p,q,aaa1,{1,1,1,1,1}];Hflechey =Expnd1[Hy,6 ,x,y,p,q,aaa1 ,{1, 1,1 ,1,1 }]; Hflechep =Expnd1[Hp,6,x,y,p,q,aaa1,{1,1,1,1,1}];Hflecheq =Expnd1[Hq,6, x,y, p,q, aaa1, {1,1 ,1,1 ,1}]; A1 = {p + y/2, q - x/2, (q - x/2)/2, -(p + y/2)/2}; B = {Hflechex ,Hflechey, Hflechep, Hflecheq } -A1;
    ***Calcul du developpement de x,y,p,q,en rho, a l'ordre6 en rho pour x y et 7 pour w
    ******************************************
    B = InputForm[Simplify[B]]t2=0;ZZ3 = Eat[t-s] . (B /.{x- rho Z1[s][[1]], y-> rho Z1[s][[2]],p->rho Z1[s][[3]],q->rho Z1[s][[4]]});Aux = Expnd1[ZZ3,3, rho, aa1,aa2,aa3 ,aa4, {1,1,1,1,1}];Z3 = Integrate[Aux, {s, 0, t}];Z3 = Simplify[(Z3) /. rho->1]; InputForm[Z3]
    Zu3s = rho Z1[s] ;BB=Expand[B];ZZ4 = Eat[t-s] . (BB /. {x->Zu3s[[1]], y->Zu3s[[2]], p-> Zu3s[[3]],q->Zu3s[[4]] });Z41 = Expnd[ZZ4,4,rho, aaa1, aaa2,aaa3, aaa4,{1,1,1,1,1}]; Z42 = Integrate[Z41[[5]],s];Int = (Z42 /. s->t)- (Z42 /. s->s1);Z4 = Simplify[Limit[Int, s1->0]]; InputForm[Z4/. rho->1]
    t2=0; BB = Expnd[B,5,x,y,p,q,aa1,{1,1,1,1,1}]; Zu3s3 = rho Z1[s]+ rho^3 ( Z3 /. t->s) ;Zu3s1 = rho Z1[s] ;ZZ5p = Eat[t-s] . (BB[[4]] /. {x->Zu3s3[[1]],y-> Zu3s3[[2]], p->Zu3s3[[3]], q->Zu3s3[[4]] }); ZZ5p1 = Eat[t-s] .( (BB[[5]] +BB[[6]])/. {x->Zu3s1[[1]], y->Zu3s1[[2]],p->Zu3s1[[3]], q-> Zu3s1[[4]] });ZZ5 = ZZ5p1+ZZ5p;Z51 = Expnd[ZZ5[[ 1]] ,5, rho, aaa1,aaa2,aaa3,aaa4, {1,1,1,1,1}]; Z52 = Expnd[ZZ5[[2]],5,rho, aaa1,aaa2,aaa3, aaa4, {1,1, 1,1, 1}];Z53 = Expnd[ZZ5[[3]] ,5, rho, aaa1,aaa2,aaa3,aaa4, {1,1,1,1,1}];Z54 = Expnd[ZZ5[[4]],5,rho, aaa1, aaa2,aaa3,aaa4,{1,1,1,1,1}];Zp5 = {Z51[[6]],Z52[[6]],Z53 [[6]],Z54[[6]]}; Zpp5= TrigReduce[Zp5]; Aux = Expand[TrigToExp[Zpp5]]; Aux1 = Integrate[Aux,s]; Zpp5 = Simplify [ExpToTrig [Aux1 ]]; Z5 = Simplify[((Zpp5)/.{ rho->1,s->t})- ((Zpp5)/.{ rho->1,s->0})];InputForm[Z5]
    t2=0;Zu3s4 =( rho Z1[s]+ rho^3( Z3 /. t->s)+ rho^4( Z4 /. t->s))/. r2->0 ; Zu3s3= ( rho Z1[s]+ rho^3( Z3 /. t->s)); Zu3s1= rho Z1[s];BB = Expnd[B,6,x,y,p, q,aa1,{1,1,1,1, 1}]; ZZ63 = Eat[t-s] . ((BB[[4]]/. r2->0) /. {x->Zu3s4[[1]], y-> Zu3s4[[2]], p->Zu3s4[[3]],q->Zu3s4[[4]] });ZZ64 = Eat[t-s] . ((BB[[5]]) /. {x->Zu3s3[[1]], y-> Zu3s3[[2]], p->Zu3s3 [[3]],q->Zu3s3[[4]] });ZZ65= Eat[t-s] . ((BB[[6]]) /. {x->Zu3s1[[1]], y-> Zu3s1[[2]], p->Zu3s1[[3]],q->Zu3s1[[4]] }); ZZ66=Eat[t-s] . ((BB[[7]]/. r2->0) /. {x-> Zu3s1[[1]],y->Zu3s1[[2]], p->Zu3s1[[3]],q->Zu3s1[[4]] }); ZZ6 = ZZ63+ZZ64+ZZ65+ZZ66; Z61 = Expnd[ZZ6[[1]],6,rho, aaa1,aaa2, aaa3,aaa4, {1,1,1,1,1}]; Z61= Simplify[Z61[[7]]]; Z62
```

= Expnd[ZZ6[[2]],6,rho, aaa1,aaa2, aaa3 ,aaa4, {1,1,1,1,1}]; Z62=Simplify[Z62[[7]]]; Z63 = Expnd[ZZ6[[3]], 6,rho, aaa1,aaa2,aaa3,aaa4, {1,1,1,1,1}]; Z63=Simplify[Z63[[7]]]; Z64 = Expnd[ZZ6[[4]], 6,rho, aaa1,aaa2,aaa3,aaa4, {1,1,1,1,1}]; Z64=Simplify[Z64[[7]]]; Z6E= {Z61,Z62, Z63,Z64}; InputForm[Z6E]

Zpp6=TrigReduce[Z6E]; Aux=Expand[TrigToExp[Zpp6]]; Aux1= Integrate[Aux,s]; Zpp6 = Simplify [ExpToTrig[Aux1]]; Z6 = Simplify[((Zpp6)/.{ rho->1,s->t})- ((Zpp6)/.{ rho->1,s->0})]; ZZ = rho Z1[t] + rhoˆ3 Z3 + rhoˆ4 Z4 + rhoˆ5 Z5+ rhoˆ6 Z6; ZZ1={Z1[t] [[1]], Z1[t] [[2]] }; ZZ3= {Z3[[1]], Z3[[2]]}; ZZ4={Z4[[1]], Z4[[2]]};ZZ5={Z5[[1]], Z5[[2]]}; ZZ6={Z6[[1]], Z6[[2]]};

********Calcul de w**********

****

Hfw7=Hflechew[[8]]/.{x->rho Z1[t][[1]],y-> rho Z1[t][[2]], p->rho Z1[t][[3]], q->rho Z1[t][[4]]}; Hfw7=Simplify[Hfw7]; Hfw7={0,0,0,0,0,0,0,Hfw7}; Hfw6= Hflechew [[7]]/. {x->rho Z1[t] [[1]], y ->rho Z1[t][[2]], p->rho Z1[t][[3]],q->rho Z1[t][[4]]}; Hfw6 =Simplify[Hfw6]; Hfw6={0,0, 0,0,0,0, Hfw6,0}; Zus=rho Z1[t]+ rhoˆ3 Z3; Hffw5=Hflechew [[6]]/. {x-> Zus[[1]],y->Zus[[2]], p->Zus[[3]],q->Zus[[4]]}; Hfw5= Expnd[Hffw5,7,rho, aa1,aa2,aa3, aa4,{1,1,1,1,1}]; Hfw5 = Simplify [Hfw5]; Zus=rho Z1[t]+ rhoˆ3 Z3 + rhoˆ4 Z4; Hffw4= Hflechew[[5]]/. {x-> Zus[[1]], y->Zus[[2]], p->Zus[[3]], q->Zus[[4]]}; Hfw4= Expnd[Hffw4,7,rho,aa1,aa2,aa3,aa4, {1,1,1,1,1}]; Hfw4= Simplify[Hfw4]; Zus=rho Z1[t]+ rhoˆ3 Z3 + rhoˆ4 Z4+rhoˆ5 Z5+ rhoˆ6 Z6; Hffw2= Hflechew[[3]]/.{x-> Zus[[1]],y->Zus[[2]], p->Zus[[3]],q->Zus[[4]]}; Hfw2= Expnd[Hffw2, 7 ,rho, aa1,aa2, aa3,aa4, {1,1,1,1,1}]; Hfw2=Simplify[Hfw2]; Hffw=Hfw2+ Hfw4+ Hfw5+ Hfw6+ Hfw7; Hfw= Hffw [[3]]+ Hffw[[5]]+ Hffw[[6]]+Hffw[[7]]+ Hffw[[8]]; Wpp7= TrigReduce[Hfw]; Aux1= Expand[TrigToExp[Wpp7]]; Aux2=Integrate[Aux1,t]; Wpp6= Simplify[ExpToTrig[Aux2]]; Aux3 = Simplify[Wpp6 -(Wpp6 /. {t-> 0})]; Aux4= Expnd[Aux3,7,rho,aa1,aa2,aa3, aa4,{1,1,1,1,1}]; Aux3= Simplify[Aux4]; W2 = Aux3[[3]]; InputForm[W2]

W4 = Aux3[[5]]; InputForm[W4] W5 = Aux3[[6]]; InputForm[W5]

W6 = Aux3[[7]];InputForm[W6] W7 = Simplify[Aux3[[8]]/. r2->0];InputForm[W7]

WW = W2+ W4+ W5+ W6+ W7;

Resultats:**********

****

InputForm[ZZ1] InputForm[ZZ3] InputForm[ZZ4] InputForm[ZZ5] InputForm[ZZ6] InputForm[W2/.rho->1] InputForm[W4/.rho->1] InputForm[W5/.rho->1] InputForm[W6 /. rho ->1] InputForm[W7/.rho->1]

Z1= {2*Cos[phi - t/2]*Sin[t/2], 2*Sin[phi - t/2]*Sin[t/2]};

Z3= {(Alpha0*(6*t*Cos[phi - t] - 6*Sin[phi] +2*Sin[phi - 2*t] + 3*Sin[phi - t] + Sin[phi + t]))/2,-(Alpha0*(-6*Cos[phi] + 2*Cos[phi - 2*t] +3*Cos[phi - t] + Cos[phi + t] - 6*t*Sin[phi - t]))/2};

Z4= ;Z5=;Z6=;

W2= (t - Sin[t])/2;

W4= (3*Alpha0*(-2*t - 4*t*Cos[t] + 4*Sin[t] + Sin[2*t]))/8;

```
W5= -(r1*(9*Cos[phi - 3*t + t1] - 85*Cos[phi - 2*t + t1] -120*Cos[phi - t + t1] +
175*Cos[phi + t + t1] + 21*Cos[phi + 2*t + t1] + 180*t*Sin[phi + t1] + 180*t* Sin[phi - t
+ t1] + 120*t*Sin[phi + t + t1]))/ 80;
W6=;W7= ;
```

Appendix 2

The next program uses the results of Appendix 1 to compute everything in the nondegenerate case where $\nabla_2^2 k \neq 0$ (or $r_2 \neq 0$). It computes first the conjugate locus just with the expansion in ρ of the exponential mapping, using the trick (consequence of Liouville's theorem) which allows to write that the equation for conjugate time is just:

$$\frac{\partial z}{\partial \varphi} \wedge \frac{\partial z}{\partial \rho} = 0,$$

in normal coordinates.

After that, it computes the expansion of the exponential mapping in suspended form.

Using this suspended form, it recomputes the approximation of the conjugate locus.

The last step is the computation of the cut locus (using the method explained in Section 3.5).

```
Z =rho Z1+rhoˆ3 Z3+rhoˆ4 Z4+rhoˆ5 Z5;
******Calcul du lieu conjugué ds le cas non degenere**
**************************************************
Zto = Z /. t->(2 Pi+to); Zto5= Expnd1[Zto,5,rho,to, aaa1,aaa2, aaa3,{1,2,1,1,1}]; Zto5=
InputForm[Simplify[Zto5]]
Zto5={(6*Alpha0*Pi*rhoˆ3 - 55*Alpha0ˆ2*Pi*rhoˆ5 - 20*Pi*r2*rhoˆ5 + rho*to +
40* Pi* rhoˆ5* to2)*Cos[phi] - 10*Pi*r2*rhoˆ5* Cos[3*phi] + 18*Alpha0ˆ 2* Piˆ2 *
rhoˆ5* Sin[ phi] + 6* Alpha0 * Pi* rhoˆ3*to*Sin[phi] + (rho*toˆ2*Sin[phi])/2 + 9*Pi*r1*
rhoˆ 4*Sin[t1] + 6*Pi*r1*rhoˆ4*Sin[2*phi + t1], -(rho*(6*Alpha0*Pi*rhoˆ2 + to)ˆ2*
Cos[phi])/2 + 9*Pi* r1* rhoˆ4* Cos[ t1] - 6*Pi*r1 *rhoˆ4 *Cos[2*phi + t1] + 6*Alpha0*
Pi*rhoˆ3* sin[phi] - 55* Alpha0ˆ2 *Pi* rhoˆ5 * Sin[phi] + 20*Pi* r2* rhoˆ5* Sin[phi] +
rho*to* Sin[phi] + 40*Pi*rhoˆ5*to2*Sin[phi] - 10* Pi*r2* rhoˆ5 *Sin[ 3*phi]};
A1 = Simplify[-((2 Pi+to)/rho) D[Zto5,to]];DZphi = D[Zto5,phi];DZr = D[Zto5,rho]
+A1; Aux = Det[{DZphi,DZr}];Aux1 = Expnd1[Aux,5,rho,to,aaa2,aaa3, aaa4, {1,2,1, 1,1}];
Aux3 = Simplify[Aux1/(2 Pi rho)];tto= (to-Aux3);tto1 = tto/. to->tto; toconj = Expnd1
[tto1, 4,rho , to, aaa1 ,aaa2, aaa3, {1,2 ,1,1 ,1} ]; toconj = InputForm[Simplify[toconj]]
toconj =Pi*rhoˆ2*(-6*Alpha0+55*Alpha0ˆ2*rhoˆ2 - 40*rhoˆ2* to2+10*rhoˆ2*r2*
Cos [2* phi] - 12*rho*r1*Sin[phi + t1]);
Conjl1 = Zto5 /. {to->toconj};Conj = InputForm[ Expnd1[Conjl1,5,rho,aaa1, aaa2,
aaa3, aaa4,{1,1,1,1,1}]; Conj = Simplify[Conjl2]]
```

```
Conj = {-20*Pi*rho^5*r2*Cos[phi]^3+3*Pi*rho^4*r1*Sin[t1], 3*Pi*rho^4* r1*Cos[t1]
+ 20*Pi*rho^5*r2*Sin[phi]^3};
Datanum1 = {Alpha0->0.5,to2->0.3, r2->0.7, t1->2.5,r1 -> 0.3,rho->0.001}; Conjnum
= Conj /. Datanum1;ParametricPlot[Conjnum, {phi,0,2 Pi}];
********Calcul de w***************
**********************************
WW=rho^2 W2+rho^4 W4+rho^5 W5+rho^6 W6;WWto = Expnd1[(WW /. t->2 Pi+to),
6, rho,to,aaa1, aaa2, aaa3, {1,2,1,1,1}]; Wto = InputForm[ Collect[Simplify[ WWto], rho]]
Wto = Pi*rho^2 - (9*Alpha0*Pi*rho^4)/ 2 + rho^6*((275*Alpha0^2*Pi)/6 - (100*Pi*
to2)/3 + 25*Pi*r2*Cos[2*phi]) - 12*Pi*rho^5*r1*Sin[phi + t1];
**********Calcul de la suspension de l'Exponentielle****
**************************************************
h = (Wto/Pi)^(1/2), sig = (s-2 h Pi)/h
**********************************
HH =rho((Pi-(9*Alpha0*Pi*rho^2)/2+rho^ 4*((275*Alpha0^2*Pi)/6 - (100*Pi*to2)/3
+ 25*Pi*r2* Cos[2*phi]) - 12*Pi*rho^3*r1*Sin[phi + t1])/Pi)^(1/2);
HH1 =InputForm[ Expnd1[HH,5,rho,aaa1,aaa2,aaa3,aaa4,{1,1,1,1,1}]]
HH1=rho - (9*Alpha0*rho^3)/4 + ((-1215*Alpha0^ 2*rho^5)/4 + (60*rho^5* ((275*
Alpha0^2* Pi)/6 - (100*Pi*to2)/3 + 25*Pi*r2*Cos[2*phi]))/Pi)/120 - 6*r1*rho^ 4*Sin[phi
+ t1];HH2 = rho+h-HH1;HH3 = HH2 /. {rho->HH2}; HH4 = Expnd1[ HH3,5,rho, h, aaa1,
aaa2,aaa3,{1,1,1,1,1}];HH5 = HH4 /. {rho->HH4};HH6 =Expnd1[ HH5,5,rho,h, aaa1,
aaa2,aaa3, {1,1,1,1,1}];RRho = InputForm[Simplify[HH6]]
RRho =h + (9*Alpha0*h^3)/4 - (499*Alpha0^2*h^5)/96 + (50*h^5*to2)/3 - (25* h^5*
r2*Cos[2*phi])/2 + 6*h^4*r1*Sin[phi + t1];SS1 = (2 Pi + to) RRho; SS2 = Expnd1[SS1,
5,h,to,aaa1, aaa2,aaa3,{1,2,1,1,1}]; SS = InputForm[ Simplify[SS2]]
SS =2*h*Pi + (9*Alpha0*h^3*Pi)/2 - (499*Alpha0^ 2*h^5*Pi)/48 + h*to + (9*Al-
pha0*h^3*to)/4 + (100*h^5*Pi*to2)/3 - 25*h^5* Pi*r2*Cos[2*phi] + 12*h^ 4*Pi*r1*Sin
[phi + t1]; SSig = InputForm[Simplify[(SS-2 h Pi)/h]]
SSig =(9*Alpha0*h^2*Pi)/2 - (499*Alpha0^2*h^4*Pi)/48 + to + (9*Alpha0* h^2*to)/
4 + (100*h^4*Pi*to2)/3 - 25*h^4*Pi*r2*Cos[2*phi] + 12*h^ 3*Pi*r1*Sin[phi + t1];TTo1
= sig+to-SSig; TTo2 = TTo1 /. {to-> TTo1};TTo2 = Expnd1[ TTo1,4,h,sig, to,aaa2,aaa3,
{1,2,2,1,1}];TTo3 = TTo2 /. {to->TTo2}; TTo4=Expnd1[ TTo3,4,h,sig,to, aaa2,aaa3, {1,2,
2, 1,1 }]; TTo = InputForm[Simplify[TTo4]]
TTo =(-9*Alpha0*h^2*Pi)/2 + (985*Alpha0^2*h^4*Pi)/48 + sig - (9*Alpha0* h^2*sig
)/4 - (100*h^4*Pi*to2)/3 + 25*h^4*Pi*r2*Cos[2*phi] - 12*h^ 3*Pi*r1*Sin[phi + t1];Zsus1
= Zto5 /. {rho->RRho, to->TTo};Zsus2 = Expnd1[ Zsus1,5,h,sig,aaa1, aaa2, aaa3, {1,2,1,1,
1}]; Zsus =InputForm[ Simplify[Zsus2] ]
Zsus ={(h*((72*Alpha0*h^2*Pi - 197*Alpha0^2*h^4*Pi - 360*h^4*Pi*r2 + 48*sig +
320*h^ 4*Pi*to2)* Cos[phi] + 6*(20*h^4*Pi*r2*Cos[3*phi] + 9*Alpha0^2* h^4 * Pi^2*
Sin[ phi ] + 12*Alpha0*h^ 2*Pi*sig*Sin[phi] + 4*sig^2*Sin[phi] + 24*h^ 3*Pi*r1*Sin[t1]
)))/48,
```

```
(h*(-6*(3*Alpha0*h^2*Pi + 2*sig)^2*Cos[phi] + 144*h^3*Pi*r1*Cos[t1] + (72* Alpha0* h^2*Pi - 197*Alpha0^2*h^4*Pi + 480*h^4*Pi*r2 + 48*sig + 320*h^4*Pi*to2 + 240*h^4* Pi*r2* Cos[ 2* phi]) *Sin[phi]))/48};
*****Recalcul du lieu conjugué, en coupant par h= Cst**
**************************************************
Aux = Det[{D[Zsus,phi], D[Zsus,sig]}];Aux1 = Expnd1[ Aux,6,h, sig,aaa1,aaa2,aaa3, {1,2, 1 ,1, 1}]; Aux2 = InputForm[Simplify[Aux1/h^2]]
Aux2 = (-3*Alpha0*h^2*Pi)/2 +(197*Alpha0^2*h^4*Pi)/48 - sig - (20*h^4* Pi*to2)/ 3 - 15*h^ 4*Pi*r2*Cos[2*phi];SigConj = InputForm[Simplify[Aux2+sig]]
SigConj =(h^2*Pi*(-72*Alpha0 + 197*Alpha0^2*h^2 - 320*h^2*to2 - 720*h^2* r2* Cos[2*phi]))/48;
Zc1 = Zsus /. {sig->SigConj};Zc2 = Expnd1[ Zc1,5,h,aaa1,aaa2,aaa3,aaa4, {1 ,1,1, 1,1}]; Zconj = InputForm[Simplify[Zc2]]
Zconj ={h^4*Pi*(-15*h*r2*Cos[phi] - 5*h*r2*Cos[3*phi] + 3*r1*Sin[t1]), h^4*Pi*
(3*r1* Cos[t1] + 20*h*r2*Sin[phi]^3)} ;
Datanum1 = {Alpha0->0.5,to2->0.3, r2->0.7, t1->2.5, r1 -> 0.3,h->0.001};Conjnum = Zconj /. Datanum1;ParametricPlot[Conjnum, {phi,0,2 Pi}];
*****Calcul du Cut-locus**************
**************************************
Er1 = (Zsus /. {phi->(phi+dphi)}) - Zsus; Er2 = Simplify[Er1];Er = InputForm[ Er= Simplify [ Er2 /(h* Sin[ dphi/2])]]
Er3 = Simplify[ Det[{{Cos[dphi/2+phi], Sin[dphi/2+phi]},Er}]];Er4 = Expnd1[ Er3,4,h, aaa1,aaa2,aaa3, aaa4,{1,1,1,1,1}];Er5 =Simplify[Er4];SigCut = InputForm[ Simplify[ 1/2(2 sig -Er5)]]
SigCut = (h^2*Pi*(-72*Alpha0+197*Alpha0^2*h^2 - 320*h^2* to2-120*h^2* r2* Cos [2 *phi] -120* h^2*r2*Cos[2*(dphi + phi)]-480*h^2*r2*Cos[dphi + 2*phi]))/48;Er6 = Simplify[Er /. {sig->SigCut}];Er7 = Expnd1[ Er6,4,h,aaa1, aaa2,aaa3,aa4, {1,1,1,1,1}]; Er8 = Det[({{ -Sin[dphi/2+phi], Cos[dphi/2+phi]},Er7})]; Er8= InputForm[Simplify[Er8]]
Er8 =-20*h^4*Pi*r2*Sin[dphi/2]^2*Sin[dphi + 2*phi]; Cutl1 = Zsus /. {sig-> (SigCut /. {dphi -> -2 phi})}; Cutl2 = Expnd1[ Cutl1,5,h,aaa1,aaa2,aaa3,aa4, {1,1,1,1,1}];Cutl = InputForm[Simplify[Cutl2]]
Cutl = {h^4*Pi*(-20*h*r2*Cos[phi] + 3*r1*Sin[t1]), 3*h^4*Pi*r1*Cos[t1]};Cutl1 = Zsus /. {sig->(SigCut/. dphi -> 0)};Cutl2 = Expnd1[ Cutl1,5,h,aaa1, aaa2,aaa3,aa4, {1,1,1, 1,1}];Cutl0 =InputForm[Simplify[Cutl2]]
Cutl0 = {-20*h^5*Pi*r2*Cos[phi]^3 + 3*h^4*Pi*r1*Sin[t1], 3*h^4*Pi* r1*Cos[t1] + 20*h^ 5*Pi*r2*Sin[phi]^3};Cutl1 = Zsus /. {sig->(SigCut /. {dphi -> (-2 phi+ Pi)})}; Cutl2 = Expnd1[Cutl1,5,h aaa1,aaa2,aaa3,aa4, {1,1,1,1,1}];CutlPi = InputForm[ Simplify[ Cutl2]]
CutlPi = {3*h^4*Pi*r1*Sin[t1], h^ 4*Pi*(3*r1*Cos[t1] + 20*h*r2*Sin[phi])};
Datanum1 = {Alpha0->0.5,to2->0.3, r2->0.7, t1->2.5,r1 -> 0.3,h- 0.001};Conjnum = Zconj /. Datanum1; Cutlnum = Cutl /. Datanum1;ParametricPlot[{Conjnum,Cutlnum}, {phi,0,2 Pi}]; Cutlnum = Cutl0 /. Datanum1; ParametricPlot[{Cutlnum}, {phi,0,2 Pi}]; Cutlnum = CutlPi /. Datanum1;ParametricPlot[{Conjnum,Cutlnum}, {phi,0,2 Pi}];
```

Appendix 3

This appendix uses the results of the program in Appendix 1 (the asymptotic expansion of the exponential mapping in terms of ρ), in order to compute everything in the degenerate case where $\nabla_2^2 k = 0$ (equivalently, $r_2 = 0$). The organization of the program is exactly the same as explained at the beginning of the previous Appendix 2.

```
Z = (rho Z1+ rhoˆ3 Z3 + rhoˆ4 Z4 + rhoˆ 5 Z5 + rhoˆ6* Z6)/.r2->0;
******Calcul du lieu conjugué ds le cas degenere**
**********************************************
Zto = Z /. t->(2 Pi+to); Zto6= Expnd1[Zto,6,rho,to, aaa1,aaa2,aaa3,{1,2,1,1,1}]; Zto6=
Simplify[Zto6]
A1 = InputForm[Simplify[-((2 Pi+to)/rho) D[Zto6,to]]];A1
A1 ={-((2*Pi + to)*(Cos[phi] + Sin[phi]*(6*Alpha0*Pi*rhoˆ 2 + to + 12*Pi* r1*
rhoˆ3* Sin[phi + t1]))), (2*Pi + to)*(-Sin[phi] + Cos[phi]*(6*Alpha0*Pi*rhoˆ2 + to +
12*Pi* r1*rhoˆ3*Sin[phi + t1]))};DZphi = D[Zto6,phi];DZr = D[Zto6,rho] +A1; Aux =
Det[{DZphi ,DZr }]; Aux1 = Expnd1[Aux,6,rho,to,aaa2,aaa3,aaa4, {1,2,1,1,1}];Aux3 =
Simplify[Aux1/(2 Pi rho)]; InputForm[Aux3]
Aux3 = 6*Alpha0*Pi*rhoˆ2 - 109*Alpha0ˆ2*Pi*rhoˆ4 + to -9*Alpha0*rhoˆ2*to +
40*Pi * rho ˆ4* to2 + 15*Pi*r32*rhoˆ5*Sin[3*phi] - 3*r1*rhoˆ3*(-4*Pi + 181* Alpha0*
Pi* rhoˆ2 + 10*to)* Sin[phi + t1] + 75*Pi*r31*rhoˆ5*Sin[phi - t31]; tto= (to-Aux3);
tto1 = tto/. to-> tto; toconj = Expnd1[tto1,5,rho,to,aaa1,aaa2,aaa3,{1,2,1,1,1}]; toconj =
InputForm[ Simplify[toconj]]
toconj =Pi*rhoˆ2*(-6*Alpha0 + 55*Alpha0ˆ2*rhoˆ2 - 40*rhoˆ2*to2 - 15*r32* rhoˆ3*
Sin[3*phi] + 3*r1*rho*(-4 + 85*Alpha0*rhoˆ2)*Sin[phi + t1] - 75*r31* rhoˆ3*Sin[phi -
t31]); Conjl1 = Zto6 /. {to->toconj}; Conjl2 = Expnd1[ Conjl1,6,rho, aaa1,aaa2, aaa3,aaa4,
{1,1,1,1,1}]; Conj = InputForm[Simplify[Conjl2]]
Conj ={-(Pi*rhoˆ4*(90*r32*rhoˆ2*Sin[2*phi] + 45*r32*rhoˆ2* Sin[4*phi] - 6*r1*
Sin[t1] + 85*Alpha0*r1*rhoˆ2*Sin[t1] + 25*r31*rhoˆ2*Sin[t31]))/2, (Pi* rhoˆ4* (-90*
r32* rho ˆ2 *Cos[ 2*phi] + 45*r32*rhoˆ2*Cos[4*phi] + 6*r1*Cos[t1] - 85*Alpha0* r1*
rhoˆ2* Cos[t1] + 25*r31 *rhoˆ2 *Cos [t31 ]))/2}; Datanum1 = {Alpha0->0.5,to2->0.3,
t1-> -2.5, r31 -> 0.7, t31 ->-1.2, r32 -> 1.3, r1 -> 0.3,rho->0.01}; Conjnum = Conj /.
Datanum1; ParametricPlot [ Conjnum ,{phi, 0, 2 Pi}];
WW = (W2 rhoˆ2 + W4 rhoˆ4 + W5 rhoˆ5 +W6 rhoˆ6 + W7 rhoˆ7)/. r2->0;WWto
= Expnd1[(WW /. t->2 Pi+to),7, rho,to, aaa1,aaa2, aaa3, {1,2,1,1,1}]; Wto = InputForm
[ Collect[ Simplify[WWto],rho]]
Wto =Pi*rhoˆ2 - (9*Alpha0*Pi*rhoˆ4)/2 + rhoˆ6*((275*Alpha0ˆ2*Pi)/6 - (100* Pi*
to2) /3) + rhoˆ5*((3*Pi*r1*to*Cos[phi + t1])/2 - 12*Pi*r1*Sin[phi + t1]) + rhoˆ7* (9*
Alpha0* Piˆ2*r1*Cos[phi + t1] + 45*Pi*r32*Sin[3*phi] + 255*Alpha0*Pi*r1*Sin[phi +
t1] - 75*Pi*r31*Sin[phi - t31]);
*********Calcul de la suspension de l'Exponentielle****
**************************************************
h = (Wto/Pi)ˆ(1/2), sig = (s-2 h Pi)/h
```

```
**********************************
HH =rho (( Pi - (9*Alpha0*Pi*rho^2)/2 +rho^ 4*((275*Alpha0^2*Pi)/6 - (100* Pi*
to2) /3 + 25*Pi*r2*Cos[2*phi]) + rho^3*((3*Pi*r1*to*Cos[phi + t1])/2 - 12*Pi* r1* Sin
[phi + t1]) + rho^5*(9*Alpha0*Pi^2*r1*Cos[phi + t1] + 45*Pi*r32*Sin[3*phi] + 255*
Alpha0*Pi* r1* Sin[ phi + t1] - 75*Pi*r31*Sin[phi - t31]))/Pi)^(1/2); HH=HH/.r2->0; HH1
= Expnd1 [ HH,6, rho,to, aaa2, aaa3, aaa4, {1,2,1,1,1}]
HH2 = rho+h-HH1; HH3 = HH2 /. {rho->HH2}; HH4 = Expnd1[HH3,6,rho,h,to, aaa2,
aaa3, {1,1,2,1,1}];HH5 = HH4 /. {rho->HH4};HH6 =Expnd1[ HH5,6, rho, h,to, aaa2,
aaa3,{1,1,2,1,1}]; RRho = Simplify[HH6]; SS1 = (2 Pi + to) RRho; SS2 = Expnd1[ SS1,
6,h,to,aaa1, aaa2,aaa3, {1,2,1,1,1}]; SS = Simplify[SS2];SSig = InputForm[ Simplify[ (SS/
h-2 Pi)]]
SSig =(9*Alpha0*h^2*Pi)/2 - (499*Alpha0^2*h^4*Pi)/48 + to + (9*Alpha0* h^2* to)
/4 + (100*h^4*Pi*to2)/3 - (3*h^3*Pi*r1*(6*Alpha0*h^2*Pi + to)*Cos[phi + t1])/2 - 45*
h^5*Pi*r32*Sin[3*phi] + 12*h^ 3*Pi*r1*Sin[phi + t1] - 39* Alpha0* h^5*Pi* r1* Sin[phi
+ t1] + 6*h^3*r1*to*Sin[phi + t1] + 75*h^5*Pi*r31*Sin[phi - t31];
TTo1 = sig+to-SSig; TTo2 = TTo1 /. {to->TTo1}; TTo2 = Expnd1[TTo1, 5,h,sig, to,aaa2,
aaa3,{1,2,2,1,1}];TTo3 = TTo2 /. {to->TTo2}; TTo4=Expnd1[ TTo3,5,h,sig,to, aaa2, aaa3,
{1,2,2,1,1}]; TTo = Simplify[TTo4];Zsus1 = Zto6 /. {rho->RRho, to-> TTo}; Zsus2 =
Expnd1[Zsus1,6,h,sig,to,aaa2,aaa3, {1,2,2,1,1}];Zsus = InputForm[ Simplify[ Zsus2 ]]
Zsus = {(h*((72*Alpha0*h^2*Pi - 197*Alpha0^2*h^4*Pi + 48*sig + 320* h^4*Pi*
to2)* Cos[phi] + 6*(3*h^3*Pi*r1*(3*Alpha0*h^2*Pi + 2*sig)*Cos[t1] + 9*Alpha0* h^5*
Pi^2 *r1 *Cos [2* phi + t1] + 6*h^ 3*Pi*r1*sig*Cos[2*phi + t1] + 9*Alpha0^2* h^4*
Pi^2* Sin[phi] + 12*Alpha0*h^2*Pi*sig*Sin[phi] + 4*sig^ 2*Sin[phi] - 120*h^5* Pi*
r32* Sin[2*phi] + 60*h^5 *Pi* r32* Sin[ 4*phi] + 24*h^3*Pi*r1*Sin[t1] - 124* Alpha0*
h^ 5* Pi*r1*Sin[t1] - 100*h^5 *Pi*r31* Sin[t31])))/48,
-(h*(6*(3*Alpha0*h^2*Pi + 2*sig)^2*Cos[phi] + 720*h^5*Pi*r32*Cos[2*phi] + 360*
h^5* Pi*r32*Cos[4*phi] - 144*h^3*Pi*r1*Cos[t1] + 744* Alpha0* h^5*Pi* r1* Cos[t1]
- 600*h^5*Pi*r31*Cos[t31] - 72*Alpha0*h^ 2*Pi*Sin[phi] + 197*Alpha0^2* h^4*Pi*
Sin[phi] - 48*sig*Sin[phi] - 320*h^4*Pi*to2*Sin[phi] + 54*Alpha0* h^ 5*Pi^2* r1*Sin[t1]
+ 36*h^3* Pi* r1* sig*Sin[t1] - 54*Alpha0*h^5*Pi^2*r1*Sin[2*phi + t1] - 36* h^ 3*
Pi*r1 *sig* Sin[2*phi + t1]))/48};
*****Recalcul du lieu conjugué, en coupant par h= Cst**
**************************************************
Aux = Det[{D[Zsus,phi], D[Zsus,sig]}];Aux1 = Expnd1[ Aux,7,h,sig, aaa1,aaa2, aaa3,
{1,2,1,1,1}]; Aux2 = Simplify[Aux1/h^2]; SigConj = Simplify[Aux2+sig];SigC = SigConj
/. sig->SigConj; SigC1 = Expnd1[SigC,5,h,sig,aaa1,aaa2,aaa3, {1,2,1,1,1}]; SigConj =
InputForm[Simplify[SigC1]]
SigConj =-(h^2*Pi*(72*Alpha0 - 197*Alpha0^2*h^2 + 320*h^2*to2 + 2880* h^3*
r32* Sin[3*phi]))/48; Zc1 = Zsus /. {sig->SigConj}; Zc2 = Expnd1[Zc1, 6,h,aaa1,aaa2,
aaa3, aaa4, {1,1,1,1,1}]; Zconj = InputForm[Simplify[Zc2]]
Zconj = {-(h^4*Pi*(90*h^2*r32*Sin[2*phi] + 45*h^2*r32*Sin[4*phi] - 6*r1*Sin[t1]
+ 31* Alpha0*h^ 2*r1*Sin[t1] + 25*h^2*r31*Sin[t31]))/2, (h^4*Pi* (-90* h^2* r32*
Cos[2*phi] + 45* h^2* r32* Cos[4*phi] + 6*r1*Cos[t1] - 31*Alpha0*h^2*r1*Cos[t1] +
```

```
25* h^2*r31* Cos[ t31] ))/2}; Datanum1 = {Alpha0->0.5,to2-> 0.3, t1->2.5,r31 -> 0.7,t31
-> -1.2, r32 -> 1.3, r1 -> 0.3,h->0.01}; Conjnum = Zconj /. Datanum1; ParametricPlot
[Conjnum, {phi,0,2 Pi}];
    *****Calcul du Cut-locus**********
    ************************************
    Er1 = (Zsus /. {phi->(phi+dphi)}) - Zsus; Er2 = Simplify[Er1]; Er = Simplify[ Er2/
(h* Sin[dphi/2])]; Er3 = Det[{{Cos[dphi/2+phi], Sin[dphi/2+phi]},Er}]; Er3= Simplify[
Er3]; Er4 = Expnd1[Er3,5,h,aaa1,aaa2,aaa3,aaa4,{1,1,1,1,1}];Er5 =Simplify[Er4]; SigCut
= Simplify[1/2(2 sig -Er5)]; SigC1 = SigCut /. sig-> SigCut;SigC2 = Expnd1[ SigC1, 5,h,
sig, aaa1,aaa2,aaa3, {1,2,1,1,1}]; SigCu = InputForm[Simplify[SigC2]]
    SigCu = -(h^2*Pi*(72*Alpha0 - 197*Alpha0^2*h^2 + 320*h^2*to2 + 360* h^3* r32*
Sin[3*phi] + 360*h^3*r32*Sin[3*(dphi + phi)] + 1080*h^3*r32*Sin[dphi + 3*phi] + 1080*
h^3* r32* Sin[2* dphi + 3*phi]))/48;Er6 =Simplify[ Er /. {sig->SigCu}];Er7 = Expnd1
[Er6,5,h,aaa1,aaa2,aaa3,aa4, {1,1,1,1,1}];Er8 = Det[({{-Sin[dphi/2+phi], Cos[ dphi/ 2+
phi]} ,Er7})]; InputForm[ Simplify[ Er8 ]]
    Er8 =120*h^5*Pi*r32*Cos[dphi/2]*Cos[(3*(dphi + 2*phi))/2]* Sin[dphi/2]^2; Cutlx1
= Zsus /. {sig->(SigCu/. {dphi -> -2 phi+Pi/3}),dphi -> -2 phi+Pi/3}; Cutlp1 = Expnd1
[Cutlx1,6,h, aaa1,aaa2,aaa3,aa4, {1,1,1,1,1}]; Cutl1 = InputForm[ Simplify[ Cutlp1 ]]
    Cutl1 ={-(h^4*Pi*(75*h^2*r32*Sin[2*phi] - 15*h^2*r32*Sin[4*phi] + 30* h^2* r32*
Cos[phi]* (Sin[3*phi] - 3*Sin[phi - (2*Pi)/3] + 3*Sin[phi + Pi/3]) - 12*r1*Sin[t1] + 62*
Alpha0*h^2*r1*Sin[t1] + 50*h^2*r31*Sin[t31]))/4, -(h^ 4*Pi*(-15*h^2*r32*(-3 + Cos
[2*phi]) *Cos[ 2*phi] + 15* h^2* r32*Cos[4*phi] - 6*r1*Cos[t1] + 31*Alpha0* h^2*r1*
Cos[t1] - 25*h^2*r31*Cos[t31] + 15*h^2*r32*Sin[phi]^2 + 15*h^2* r32* Sin[phi]* Sin
[3*phi] - 45* h^2* r32* Sin[phi]* Sin[phi - (2* Pi) /3] + 45*h^2* r32* Sin[phi]* Sin[phi
+ Pi/3]))/2}; Cutlx2 = Zsus /. {sig->(SigCu/. {dphi -> -2 phi+Pi/3+ 2 Pi/3}),dphi -> -2 phi
+Pi/3+ 2 Pi/3}; Cutlp2 = Expnd1[ Cutlx2,6,h, aaa1,aaa2, aaa3,aa4, {1,1,1,1,1}]; Cutl2 =
InputForm[Simplify[Cutlp2]]
    Cutl2 = {-(h^4*Pi*((-6 + 31*Alpha0*h^ 2)*r1*Sin[t1] + 25*h^2*r31*Sin[t31]))/2, -
(h^4 *Pi* (90* h^2* r32*Cos[2*phi] + (-6 + 31*Alpha0*h^2)*r1*Cos[t1] - 5*h^2*(9*r32
+ 5*r31* Cos[t31])))/2};
    Cutlx3 = Zsus /. {sig->(SigCu/. {dphi -> -2 phi +Pi/3+ 4 Pi/3}),dphi -> -2 phi +Pi/3+
4 Pi/3};Cutlp3 = Expnd1[Cutlx3,6,h,aaa1,aaa2,aaa3,aa4,{1,1,1,1,1}];Cutl3 = InputForm
[Simplify[ Cutlp3]]
    Cutl3 = {-(h^4*Pi*(75*h^2*r32*Sin[2*phi] - 15*h^2*r32*Sin[4*phi] + 30*h^2* r32*
Cos[phi]* (Sin[3*phi] - 3*Sin[phi - (10*Pi)/3] + 3*Sin[phi + (5*Pi)/3]) - 12*r1* Sin[t1]
+ 62*Alpha0*h^2*r1*Sin[t1] + 50*h^2*r31*Sin[t31]))/4, -(h^4* Pi* (-15* h^2* r32* (-3
+ Cos[2*phi])*Cos[2*phi] + 15*h^2*r32*Cos[4*phi] - 6*r1*Cos[t1] + 31* Alpha0* h^2*
r1* Cos[ t1] - 25*h^2*r31*Cos[t31] + 15*h^2*r32*Sin[phi]^2 + 15*h^2* r32* Sin[phi]
*Sin[3*phi] - 45* h^ 2* r32* Sin[phi]* Sin[phi - (10* Pi)/3 ] + 45*h^2* r32* Sin[phi]*
Sin[phi + (5*Pi)/3]))/2};
    Cutlx0 = Zsus /. {sig->(SigCu/. dphi -> 0), dphi->0}; Cutlp0 = Expnd1[ Cutlx0,6,h,
aaa1, aaa2,aaa3,aa4,{1,1,1,1,1}];Cutl0 = InputForm[Simplify[Cutlp0]]
```

```
Cutl0 = {-(hˆ4*Pi*(90*hˆ2*r32*Sin[2*phi] + 45*hˆ2*r32*Sin[4*phi] - 6*r1*Sin[t1]
+ 31*Alpha0*hˆ 2*r1*Sin[t1] + 25*hˆ2*r31*Sin[t31]))/2, (hˆ4*Pi* (-90*hˆ2*r32*
Cos[2* phi] + 45*hˆ2*r32*Cos[4*phi] + 6*r1*Cos[t1] - 31*Alpha0*hˆ2*r1*Cos[t1] +
25* hˆ2*r31* Cos[ t31 ]))/ 2}; Cutlxp0 = Zsus /. {sig->(SigCu/. dphi -> Pi), dphi->Pi};
Cutlpp0 = Expnd1[ Cutlxp0,6,h, aaa1,aaa2,aaa3,aa4, {1,1,1,1,1}]; Cutlp0 = InputForm
[Simplify[ Cutlpp0]]

Cutlp0 ={(hˆ4*Pi*(-30*hˆ2*r32*Sin[2*phi]+15*hˆ2*r32*Sin[4*phi]+6*r1* Sin[t1]
- 31*Alpha0*hˆ 2*r1*Sin[t1] - 25*hˆ2*r31*Sin[t31]))/2, -(hˆ4* Pi*(30* hˆ2*r32*
Cos[2*phi]+15*hˆ2*r32*Cos[4*phi]-6*r1*Cos[t1]+31*Alpha0*hˆ2*r1*Cos[t1]-25*
hˆ2*r31* Cos[t3 1 ]) )/2} ; Datanum1 = {Alpha0->0.5,to2-> 0.3, t1->2.5,r31 -> 0.7,t31
-> -1.2, r32 -> 1.3,r1 -> 0.3,h->0.01 }; Conjnum = Zconj /. Datanum1;Cutlnum0 = Cutl0
/. Datanum1; Cutlnump0 = Cutlp0 /. Datanum1; Cutlnum1 = Cutl1 /. Datanum1; Cutl-
num2 = Cutl2 /. Datanum1; Cutlnum3 = Cutl3 /. Datanum1; ParametricPlot[ {Conjnum,
Cutlnum1, Cutlnum2,Cutlnum3}, {phi,0,2 Pi}]; ParametricPlot[{Cutlnum0,Cutlnump0},
{phi,0,2 Pi}];
```

References

1. Agrachev, A. A.: Methods of control theory in nonholonomic geometry, in: *Proceedings ICM-94*, Birkhäuser, Zürich, 1995.
2. Agrachev, A. A.: Exponential mappings for contact sub-Riemannian structures, *J. Dynamical and Control Systems* **2**(3) (1996), 321–358.
3. Agrachev, A. A., Bonnard, B., Chyba, M. and Kupka, I.: Sub-Riemannian sphere in Martinet flat case, in: *COCV / S1*, Dec. 1997, pp. 377–448.
4. Agrachev, A. A., Chakir, H. and Gauthier, J. P.: Sub-Riemannian metrics on R^3, in: *Geometric Control and Nonholonomic Mechanics*, Proc. Canadian Math. Soc. 25, 1998, pp. 29–78.
5. Agrachev, A. A., Chakir, H., Gauthier, J. P. and Kupka, I.: Generic singularities of sub-Riemannian metrics on R^3, *C.R. Acad. Sci. Paris Sér. I* **322** (1996), 377–384.
6. Arnold, V., Varchenko, A. and Goussein-Zadé, S.: *Singularités des applications différentiables*, Mir, Moscow, French translation, 1986.
7. Baldé, M.: Remarks on some isoperimetric problems, to appear.
8. Carathéodory, C.: *Calculus of Variations and Partial Differential Equations of the First Order*, 3rd edn, Chelsea Publishing Company, NY 10016, 1989.
9. Chakir, H., Gauthier, J. P. and Kupka, I.: Small sub-Riemannian balls on R^3, *J. Dynamical and Control Systems* **2**(3) (1996), 359–421.
10. Chyba, M: Exponential mapping, spheres and wave fronts in sub-Riemannian geometry: The Martinet case, PhD Thesis, University of Burgandy, 1997.
11. Golubitskii, M. and Guillemin, V.: *Stable Mappings and Their Singularities*, Springer-Verlag, New York, 1973.
12. Kobayashi, S. and Nomizu, K.: *Foundations of Differential Geometry*, Wiley, 1969.
13. Kupka, I.: Géométrie sous-Riemannienne, *Séminaire BOURBAKI*, 48ème année, 1995–96, 817.
14. Mather, J.: Stability of C^∞ mappings, I–VI, *Ann. of Math.* **87** (1968), 89–104; **89** (1969), 254–291; *Publ. Sci. IHES* **35** (1969), 127–156; **37** (1970), 223–248; *Adv. in Math.* **4** (1970), 301–335; *Lecture Notes in Math.* **192** (1971), 207–253.
15. Montgommery, R.: Isholonomic problems and some applications, *Comm. Math. Phys.* **128** (1990), 565–592.
16. Pontriaguine, L., Boltianski, V., Gamkrelidzé, R. and Mitchenko, E.: *La théorie Mathématique des Processus Optimaux*, Mir, Moscow, French translation, 1974.

17. Steenrod, N.: *The Topology of Fiber Bundles*, Princeton University Press, New Jersey, 1951.
18. Whitney, H.: On singularities of mappings of Euclidian spaces, I–II, in: *Symposium Internacional de Topologia Algebraica, Mexico City, 1958; Ann. of Math.* **62**(3) (1955).